Organosilicon Radical Cations

Hans Bock* and Bahman Solouki

Chemische Institute der Universität Frankfurt, Marie-Curie-Str.11, D 60439 Frankfurt, Germany

Received February 21, 1995 (Revised Manuscript Received May 4, 1995)

Contents

I. The Molecular State Approach to Silicon Compounds

The fascination of organosilicon radical cations, i.e. positively charged molecular ions with doublet ground states readily generated because of the low effective nuclear charge of the Si centers, has stimulated two reviews in 1989, one comprehensive[1] and the other based on a lecture in Hawaii.[2]

Today, more than 6 years later, a further progress report is justified. We will have to begin again with the basics of molecular states, the building blocks of the space-age chemist. Even if interested predominantly in preparative chemistry, a chemist will profit considerably by looking at instrumental analysis spectra from the point of view that these represent "molecular state fingerprints":[1] In addition to the analytical "ear-tagging", such measurements afford valuable but often unused information about the compound investigated, including the energies and the symmetries of its various states, as well as the energy-dependent electron distribution over the effective nuclear potentials. Let us, therefore, tentatively take a "molecular-state magnifying glass" (Figure 1) and examine the relation between structure and energy for selected compounds of silicon.[2]

Molecular states are—as documented, for example, by photochemical synthesis steps or by redox reactions—the real components of chemistry and can be ordered with respect to both energy[3,4] (Figure 2) and time scales[4,5] (Figure 3).

For closer elaboration of the abundant radical cation states on energy and time scales (Figures 2 and 3) photoelectron[1-3,6,7] and electron spin resonance (ESR/ENDOR)[8] spectroscopic techniques are most valuable and have complementary time scales (Figure 3): "Vertical" ionization energy patterns are measured with a time resolution of less than 10^{-15} s and, therefore, can be correlated to the eigenvalues calculated for the neutral molecule by applying Koopmans' theorem, $IE_n^v = -\epsilon_j^{SCF}$.[1-3] In contrast, ESR/ENDOR signal patterns are recorded "adiabatically" with a considerably smaller time resolution of $>10^{-8}$ s, that is, long after the activation of molecular dynamics at about 10^{-13} s. The spin populations ϱ_μ detected for the individual radical ion centers μ can be rationalized according to the McConnell relation, $\varrho_\mu \propto c_{j\mu}^2$, by comparison with the calculated squared orbital coefficients $c_{j\mu}^2$.[8] The two measurement techniques complement each other for radical cation investigation because of their different time resolution and together, when combined with approximate hypersurface calculations,[9] allow reliable estimates of structural changes in molecules M on adiabatic one-electron oxidation $M \rightarrow M^{\bullet+} + e^-$.

Numerous molecular state data (Figure 2), especially those for radical cations, can be discussed advantageously on the basis of a qualitative molecular state model (1) supported by quantum-chemical calculations, which only consider the topological connection between centers, the symmetry of their spatial arrangement, their effective nuclear potentials, and the resulting electron distribution:[1-4]

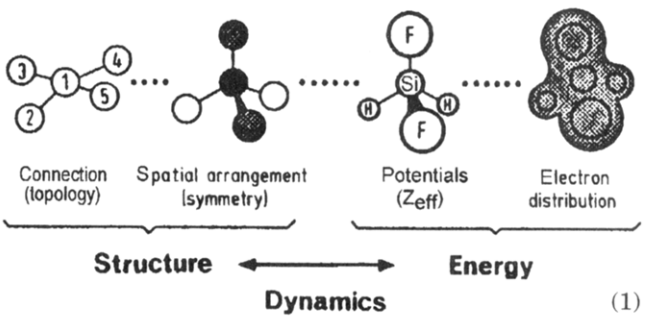

(1)

0009-2665/95/0795-1161$15.50/0

Hans Bock obtained his Ph.D. in 1958 from the Ludwigs-Maximilians-University in Munich, submitting a thesis on reactions of the rocket fuel hydrazine, and his habilitation in 1964 was based on investigations concerning relations between color and constitution of azo compounds. In the following 3 years as a visiting fellow at the Federal Institute of Technology in Zürich, the three-volume book *The HMO Model and its Application* was compiled under the guidance of his mentor and friend Edgar Heilbronner and later translated into English, Japanese, and Chinese. In 1968 he received the Chemistry Award of the Academy of Science in Göttingen and the offer of an inorganic professorship at the Johann-Wolfgang-Goethe University of Frankfurt. Preparative nonmetal chemistry, in combination with physical measurements and quantum-chemical calculations, has remained the trademark of his research group: Short-lived molecules, some of them found in interstellar space, are generated under nearly unimolecular conditions and identified by their PE spectroscopic ionization fingerprints. Radical ions and their ion pairs in aprotic solution are characterized by their ESR/ENDOR signal patterns. Well over 300 crystals have been grown since 1990 and their structures determined to gather information on both molecular distortions due to charge perturbation or steric overcrowding and static aspects of molecular self-organization. Professor Bock, a dedicated university teacher, has won numerous honors, among them the Frederic Stanley Kipping Award of the American Chemical Society and the Wilhelm Klemm Award of the German Chemical Society. The Universities of Hamburg and of Montpellier have bestowed honorary Ph.D. degrees on him. Since 1977 he has been an External Scientific Member of the Max Planck Society and since 1981 an Adjunct Professor of The University of Michigan, Ann Arbor, MI. Professor Bock also holds Memberships to the Academies of Sciences in Mainz, Göttingen, and München, as well as to the Leopoldina in Halle.

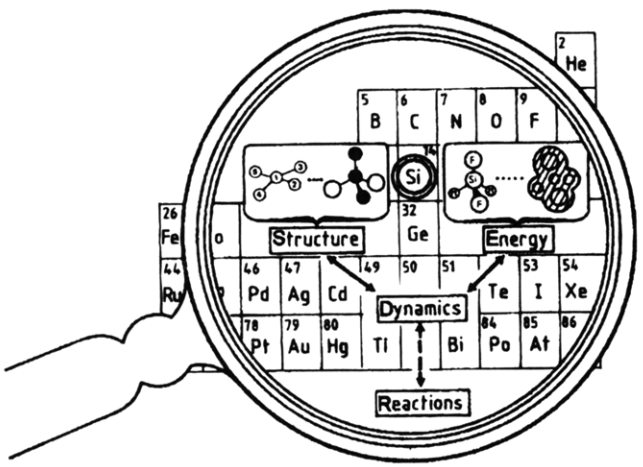

Figure 1. "Molecular-state magnifying glass" for the silicon chemist.

Despite the rather drastic simplifications within such a qualitative approach, however, the calculations accentuate that each molecular state defined must possess an individual structure, and that changes in energy and charge distribution (Figure 2) will always provoke structural changes through the inherent molecular dynamics (1) within the complexity of the $3N - 6$ degrees of freedom.[9]

Bahman Solouki was born in Iran and, being a member of the Bahaií faith, is engaged in the case of world unity. He obtained his Ph.D. in 1974 from the Johann Wolfgang Goethe University in Frankfurt, submitting a thesis on photoelectron–spectroscopic and quantum-chemical investigations of molecules containing S···X multiple bonds. Since then he has generated numerous interstellar molecules, often for the first time, and characterized them by recording and calculating their radical cation state "ionization fingerprints." His contributions to silicon chemistry comprise the first investigation of silabenzene, silaethylene, $R_3SiC{\equiv}P$, and $SiCl_2$ as novel molecules and recording and assignment of PE spectra of silicon compounds, including, more recently, 1,2-disila-*closo*-dodecaborane. He participated in the development of "photoelectron-spectroscopic gas analysis", a most valuable method used to screen and optimize heterogeneously catalyzed reactions of industrial interest. Since 1990 he has been Academic Director of the Institute of Inorganic Chemistry at Frankfurt University and, accordingly, responsible for both the advanced inorganic laboratory course and the environmentally safe disposal of used chemicals.

In conclusion, the general point of view is put forward that molecules act as "self-dedicated computers" "printing out" measurement data which provide complete, (self-consistent) and completely correlated solutions of the Schrödinger equation.[3] The follow-up question, whether to measure or to calculate, resulting from the rapid development of numerical quantum mechanics, is best answered with reference to how successful and stimulating the combination of the two proves to be. Among the numerous measurement techniques available, the above mentioned (Figure 2) photoelectron (PE)[1,6] and electron spin resonance (ESR/ENDOR)[8] spectroscopy have proven to be especially informative for preparatively oriented molecular state investigations (Figures 2 and 3). The assignment of "vertically" recorded ionization energy patterns via Koopmans' correlation, $IE_n^{v} = -\epsilon_j^{SCF}$, with SCF eigenvalues allows PE spectrometers to be regarded as "eigenvalue meters". ESR/ENDOR instruments, which record signal patterns adiabatically, on the other hand might be considered as "π-eigenfunction-squared meters",[2] because the detected π-spin population ϱ_μ^π of radical centers can be correlated via $\Psi_\pi^2 \rightarrow \sum c_{\pi\mu}^2$ with the squared orbital coefficients.

The provocative question of how a preparative silicon chemist can profit by looking at molecular state fingerprints comes at a time, when at least one chemical publication appears in every one of the 525 600 min of a 365-day year and can be best answered by examining the information revealed by spectroscopic band or signal patterns. Not only can

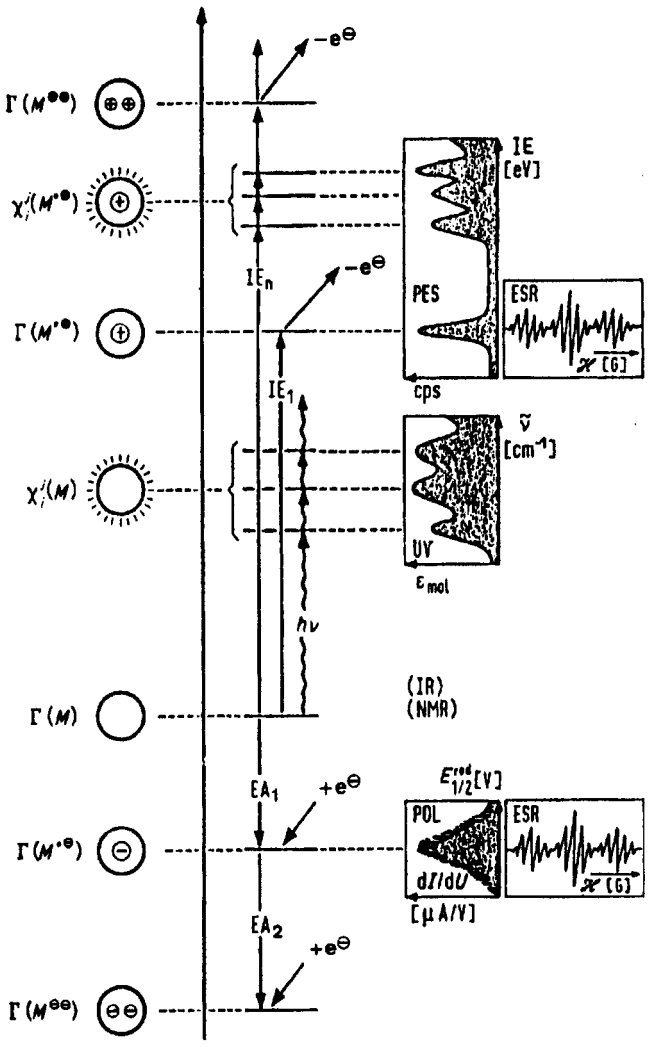

Figure 2. Schematic energy scale for electronic ground (Γ) and exited (χ_j^i) states of a neutral molecule M, its radical cation $M^{\bullet+}$ or dication M^{2+} generated by ionization or oxidation and its radical anion $M^{\bullet-}$ and dianion M^{2-} resulting from electron insertion. Representative measurement methods used in many investigations are NMR, IR, UV, PE, ESR, and ENDOR spectroscopy as well as polarography (POL) or cyclic voltammetry.

the respective compounds be identified and characterized from these patterns but the information is also of considerable benefit in molecular-state-guided planning and evaluation of experiments as is outlined in this review for the exemplary case of organosilicon radical cations.

II. Introductory "Classic" Examples

An examination of the literature for the years 1989 to 1994 presented in sections III and IV under the various aspects specified should be preceded by some selected representative examples to introduce the basics needed for comparison and rationalization. With their landmark character, the examples include some historical aspects such as (1) the discovery of the $\sigma_{SiSi}/\sigma_{SiSi}$ ionization band splitting in the PE spectra of polysilanes in 1971,[10,11] (2) the ^{29}Si ENDOR spectroscopy established in 1983,[12] (3) the generation of unstable molecules under unimolecular conditions in the gas phase comprising $H_5C_6N{\equiv}Si$ in 1985,[13] still uniquely exhibiting a triply bonded Si of coordination number 1, (4) some of the useful theoretical principles for the discussion of the experimental results such as substituent perturbation, and (5) an overview on the largely satisfactory reproduction of both energy values and structural details by semiempirical calculations.[1,2]

1. Electron Delocalization in Polysilane Radical Cations

One of the most informative ionization fingerprint comparisons is that of the isovalence electronic molecules disilane and ethane (Figure 4).

From comparison of the He I PE spectra[1,2] (Figure 4) it is possible to see that both molecules each have 14 valence electrons, giving rise to seven $M^{\bullet+}$ states, of which six are within the He I measurement range up to 21.21 eV. The difference in the effective nuclear charges of individual centers (1),[3] here $Z_{eff}(Si) <<< Z_{eff}(C)$,[2] which is extremely important for specific $M^{\bullet+}$ states, shows the tremendous shifts of 3.6 eV = 347 kJ mol^{-1} for the $3s_{Si} \leftarrow 2s_C$ ionizations and of 3.0 eV = 290 kJ mol^{-1} for the $\sigma_{SiSi} \leftarrow \sigma_{CC}$ ionizations. In both radical cations, the formerly degenerate σ_{EH} ($E_g + E_u$) states exhibit Jahn/Teller distortions between 0.3 and 0.8 eV (Figure 4, J/T), indicating a $D_{3d} \rightarrow C_{2h}$ structural change. The biggest difference, however, between the two isoelectronic radical cations is the low-energy ground state of $H_3Si{-}SiH_3^{\bullet+}$ with predominant positive charge delocalization in the SiSi bond.

As expected from the ground state Γ(SiSi) of $H_3Si{-}SiH_3^{\bullet+}$ at only IE_1^v = 10.53 eV (Figure 4), the SiSi-bond-dominated $M^{\bullet+}$ states of linear polysilanes Si_nH_{2n+2} are so easily ionized that the corresponding PE bands are lowered out of the σ_{SiH} ionization area betwen 11 and 14 eV (Figure 5).[1,2,11] The splitting—somewhat unsymmetrical due to the considerable density of symmetry-equivalent states at higher energy—convincingly demonstrates the electron hole delocalization along the Si_n molecular backbone.

The photoelectron spectra[1,2,10] of permethylated polysilanes also exhibit characteristic band patterns in the low-energy region up to 10 eV, which have been assigned analogously (Figures 5 and 6) to radical cation states with predominant SiSi framework contributions. For rationalization, a linear combination of bond orbitals (LCBO) based on the molecular orbital (MO) approach provides a fully occupied energy-level scheme (Figure 6) with eigenvalues, $\epsilon_j^{HMO} = \alpha_{SiSi} + x_j^{HMO}\beta_{SiSi/SiSi}$, which on correlation with the PE spectroscopic vertical ionization energies IE_n^v (eV) yield a satisfactory linear regression. The center of the energy level scheme is the Coulomb term α_{SiSi} = 8.69 eV, which represents the first ionization energy of hexamethyldisilane. Its gradient defines the interactions parameter $\beta_{SiSi/SiSi} \approx 0.5$ eV.

The applicability of a topological LCBO–MO model[1,2,10] to rationalize σ_{SiSi} ionization patterns of polysilanes Si_nR_m is further supported by the reproducibility of numerous experimental details: To begin with, all "alternating"[3,14] chain polysilanes as well as the six-membered ring show approximately equally spaced splitting patterns around α_{SiSi}. Expectations from an isoconjugate perimeter model[3,4] are also met by the spectroscopic observations that

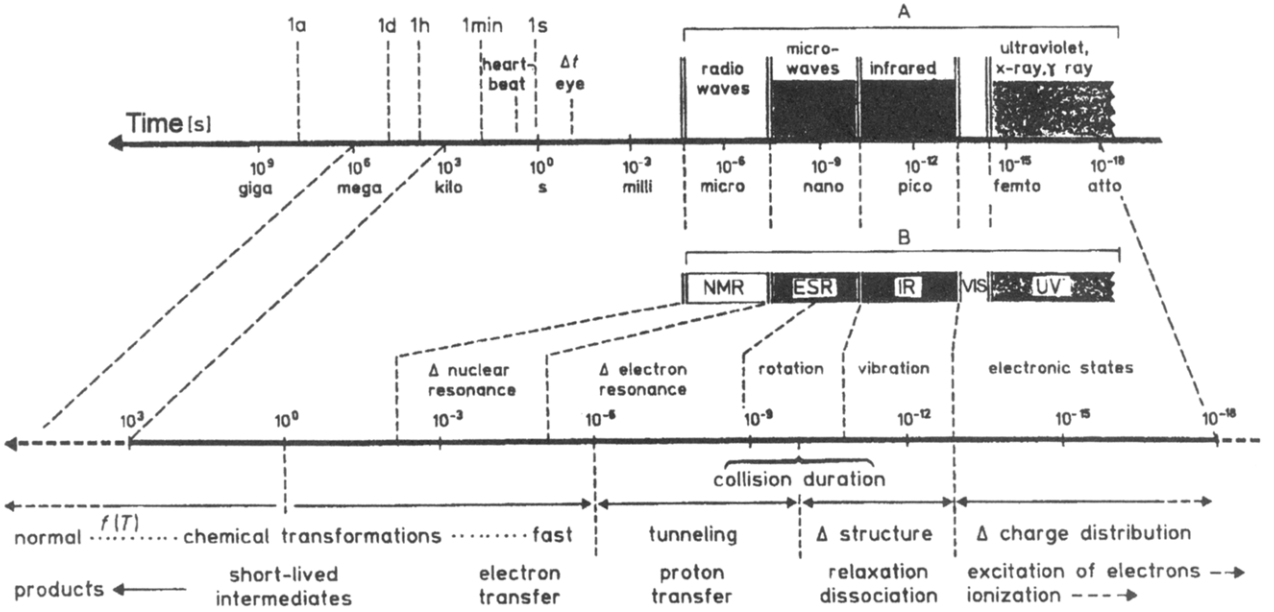

Figure 3. Schematic time scale for molecular states and their changes (in seconds).

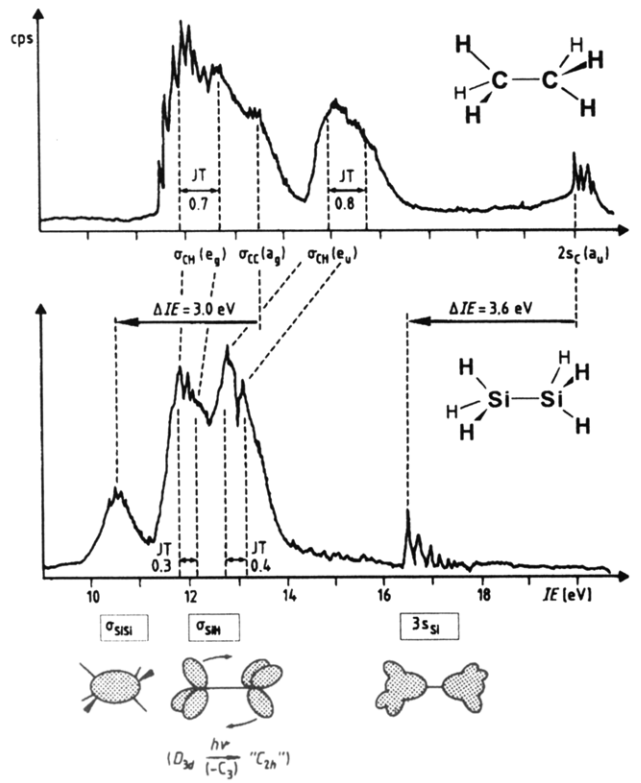

Figure 4. Comparison of the He I PE spectra of ethane and disilane, exhibiting Jahn/Teller splitting (J/T) of their $M^{\bullet+}$ (e) states with predominant contributions (□) to positive hole delocalization (cf. the text).

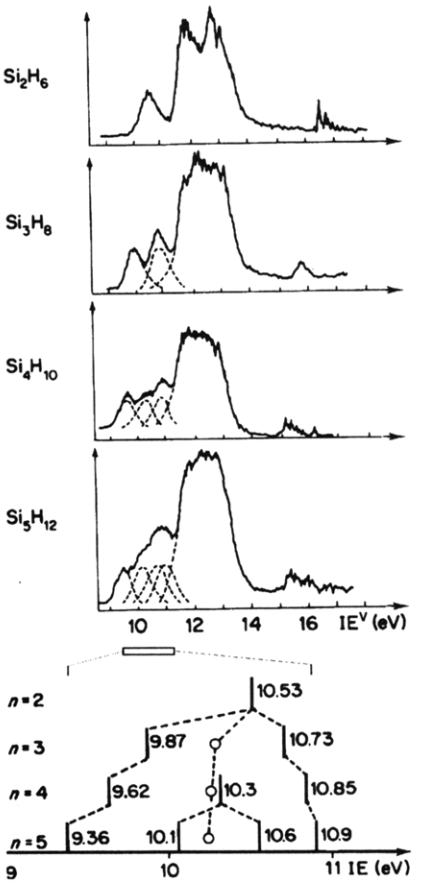

Figure 5. He I spectra of open-chain silanes Si_nH_{2n+2} (n = 2–5) with enlarged $\sigma_{SiSi}/\sigma_{SiSi}$ splitting patterns between 9 and 11eV (cf. the text).

the highest SiSi ionization energies, IE_5^v = 9.80 eV and IE_6^v = 9.78 eV, of the five- and six-membered rings are almost identical (Figure 6) as predicted from their identical eigenvalues, $\epsilon_j^{HMO} = \alpha + 2\beta$,[3] and that some of their lower-energy ionizations are predicted and found to be pairwise degenerate.[1-3]

Altogether, the 21 IE_n values measured 20 years ago for polysilanes were fit into the simple topological LCBO–MO model for their radical cation states and yielded the experimental Coulomb and interaction parameters, α_{SiSi} = 8.7 eV and $\beta_{SiSi/SiSi} \approx$ 0.5 eV. Comparison of the latter with the analogous data for π interaction in the $M^{\bullet+}$ states of linear polyenes, $\beta_{C=C/C=C} \approx$ 1,2 eV,[15] further confirms the—albeit less effective—delocalization of the positive charge over the SiSi skeleton in the radical cations of permethylated polysilanes. This stabilization of charges resulting in one-electron ejection from the organosilicon compounds with several Si centers of low effective nuclear charge (1), vice versa, causes the rather low first vertical ionization energies measured

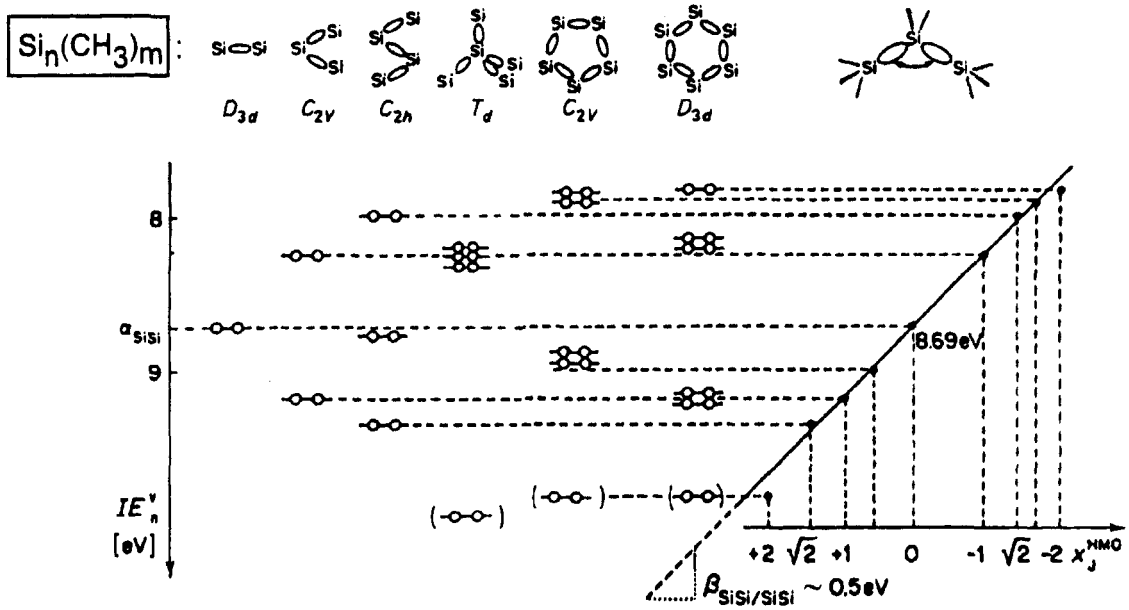

Figure 6. SiSi bond ionization patterns, IE_n^v (eV), of permethylated linear or cyclic polysilanes $Si_n(CH_3)_{2n+2}$ or $Si_n(CH_3)_{2n}$ and their correlation with topological eigenvalues $x_j^{HMO}(\beta_{SiSi/SiSi})$. (Values in brackets denote ionization in areas of overlapping bands; cf. the text).

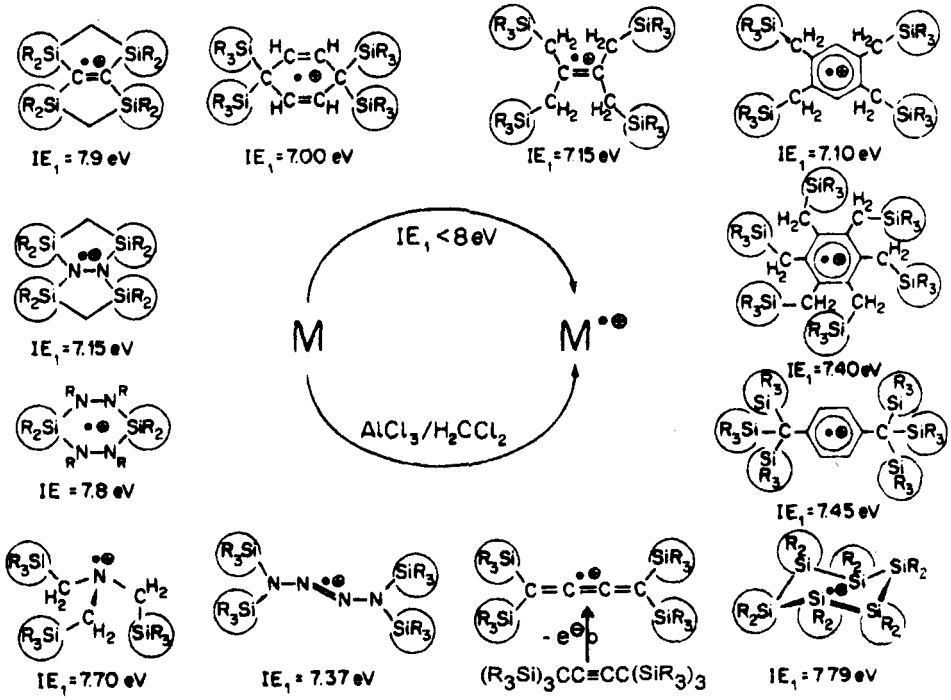

Figure 7. Prototype organosilicon radical cations, generated by $AlCl_3/H_2CCl_2$ oxidation from neutral parent compounds, exhibiting vertical first ionization energies below 8 eV and characterized by their ESR or ENDOR spectra (Figure 8).

(Figures 3–5) and, therefore, are the starting point for generation of organosilicon radical cations in solution also.[16,17]

2. ^{29}Si ENDOR Spectroscopy of Organosilicon Radical Cations

Since the oxygen- and water-free, easy-to-handle, and highly selective one-electron oxidation system $AlCl_3/H_2CCl_2$ was discovered 20 years ago,[18] a multitude of organosilicon radical cations, $M^{+\bullet}$, have been generated from polysilanes, from R_3SiCH_2-substituted π systems and amines, from R_3Si-substituted hydrazines and tetrazenes, or from persilylated dimethylacetylene (Figure 7).[16] Cyclovoltammetric measurements[17] approximate an (irreversible) potential of about +1.7 V for this couple, which corresponds to a first vertical ionization energy of the respective organosilicon molecule below 8 eV.[16] Thus, straightforward predictions of feasible one-electron oxidations by $AlCl_3$ in H_2CCl_2 solution to generate the respective radical cations from examination of the numerous literature photoelectron data can easily be made.

Even high-resolution ESR spectra hardly can resolve the sometimes enormous number of lines and intensity differences especially in fluctuating organosilicon radical cations.[16] As another example (Figure 7), 1,4,5,8-tetrakis(trimethylsilyl)-$\Delta^{4a(8a)}$-oc-

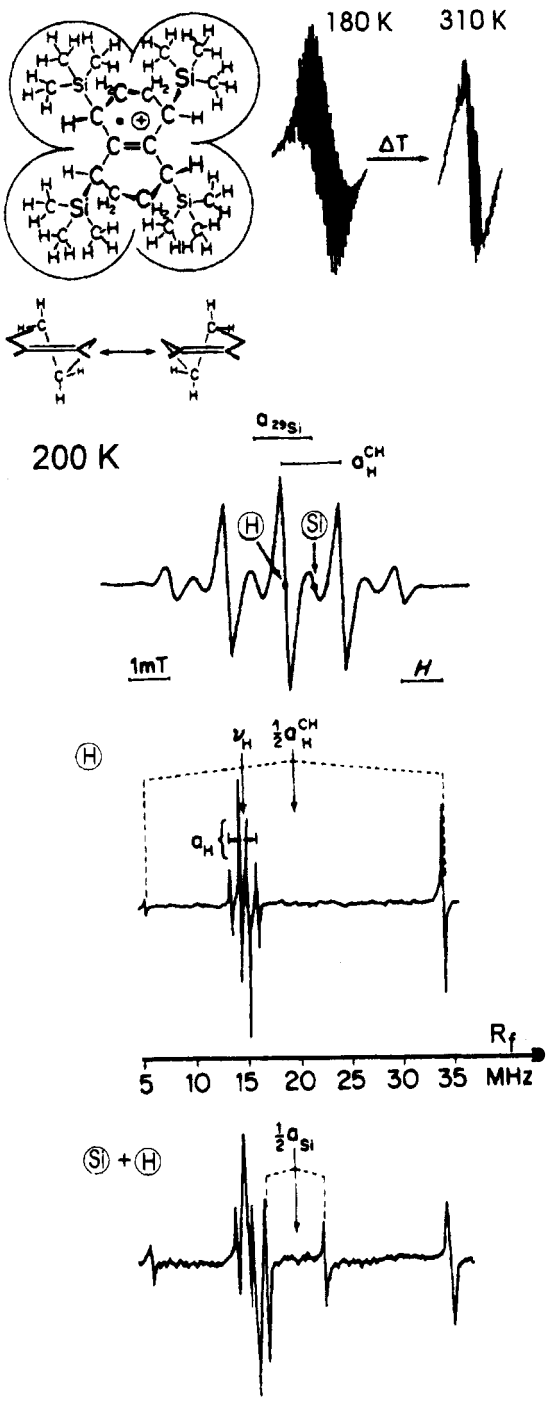

Figure 8. ESR and ENDOR spectra of 1,4,5,8-tetrakis-(trimethylsilyl)-1,2,3,4,5,6,7,8-octahydronaphthalene radical cation generated with $AlCl_3/H_2CCl_2$. The temperature depencence of the ESR line splitting between 180 and 300 K is due to flip-flops of the six-membered rings. H and Si indicate the points of ESR saturation for the additional NMR sweep to record the $^1H + ^{29}Si$ ENDOR spectra (cf. the text).

talin radical cation (Figure 8) has been selected, for which a total of $\prod(2n_N I_N + 1) = 5 \times 5 \times 5 \times 37 + 2(5 \times 5 \times 5 \times 37) = 13\,875$ lines are predicted due to four sets of each 4, 4, 4, and 36 equivalent ^1H nuclei and one ^{29}Si nucleus ($I_{Si} = 1/2$, natural abundance 4,70%): Of the 925 lines expected alone for the ESR central region with no silicon hyperfine splitting, only about 50 can be distinguished at 180 K[12,18] (Figure 8, 180 K). The sterically shielded radical cation is persistent even at room temperature and exhibits ($-H_2CCH_2-$)-wagging vibrations. The ESR spectrum (Figure 8, 200 K) is dominated by the quintet signal from the four $H(CSiR_3)$ hydrogens: the satellites flanking both sides of each line arise from the corresponding quintet of a radical with a single ^{29}Si nucleus present in $4.170 \times 4 = 18.8\%$ natural abundance. Upon irradiation with an additional frequency[8] into the ^1H main signal, the ^1H ENDOR spectrum results (Figure 8, H), and upon saturation of the satellite signal the $^{29}Si + ^1H$ ENDOR spectrum can be observed (Figure 8, Si + H). The resulting advantages of using ENDOR spectroscopy are tremendous: The ESR complexity of 13 875 signals is reduced to just single line pairs for each set of equivalent nuclei, N; i.e. altogether there are $2N = 2 \times 5 = 10$ lines for our example, which according to the ENDOR resonance condition, $\nu_{ENDOR} = |\nu_N \pm a_N/2|$, are centered either around the nuclear frequency ν_N with a separation a_N, or—for $a_N/2 > \nu_N$—around $a_N/2$ with a separation $2\nu_N$ (Figure 8). The gain in resolution when going from ESR to ENDOR amounts to several orders of magnitude[8,12] and allows the determination of the hyperfine coupling constants even when the ESR spectrum is resolved incompletely or not at all. From TRIPLE resonance measurements, the relative signs of the ^1H and ^{29}Si couplings can be determined,[8,12] providing complete information on the ESR multiplet signal pattern of $((H_3C)_3Si)_4C_{10}H_{12}^{\bullet+}$ (Figure 8):

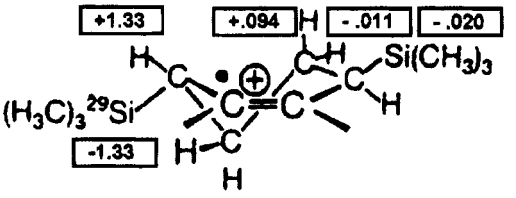

(2)

Since the ^{29}Si nucleus has a negative magnetic moment, the positive s-spin density at the Si center demonstrated in this radical cation corresponds to a negative ^{29}Si coupling. Easy ENDOR monitoring of the hyperfine splittings as a function of experimental parameters reveals that in the tetrakis(trimethylsilyl)-octahydronaphthalene radical cation the coupling constant α^{29}_{Si} decreases and α_H^{CH} increases with increasing temperature:[12] For the molecular dynamics on the ENDOR time scale it follows, therefore, contrary to steric requirements, that the $H(CSiR_3)$ hydrogens have a higher probability of being located in the axial position, favoring hyperconjugative spin transfer.[12]

Summarizing, the ENDOR effect of the ^{29}Si nuclei in organosilicon radical cations is in general comparable with that of the hydrogens. The "quantum jump" increase in NMR resolution[8] yields considerable information (2) and contributes to a better understanding of the structure and dynamics of organosilicon radical cations in solution, which can be generated in large numbers from π systems substituted with R_3SiCH_2 donor groups using the highly selective, powerful, and oxygen-free one-electron transfer system $AlCl_3/H_2CCl_2$ (Figure 7) with its added advantage of being "ENDOR capable".

3. Gas Analysis by Ionization Fingerprints: $H_5C_6N{\equiv}Si$

The assumption that the main-group elements of the higher periods exhibit only limited ability to form $p_\pi p_\pi$-multiple bonds, the so-called "double bond rule", has been disproved again and again, even for organosilicon compounds:[19] Numerous short-lived parent molecules such as silabenzene[1,2,20,21] or silaethene[1,2,20,21] can be generated selectively under unimolecular gas phase conditions, which can be optimized using photoelectron spectroscopic ionization "fingerprints" (sections I and II.1):

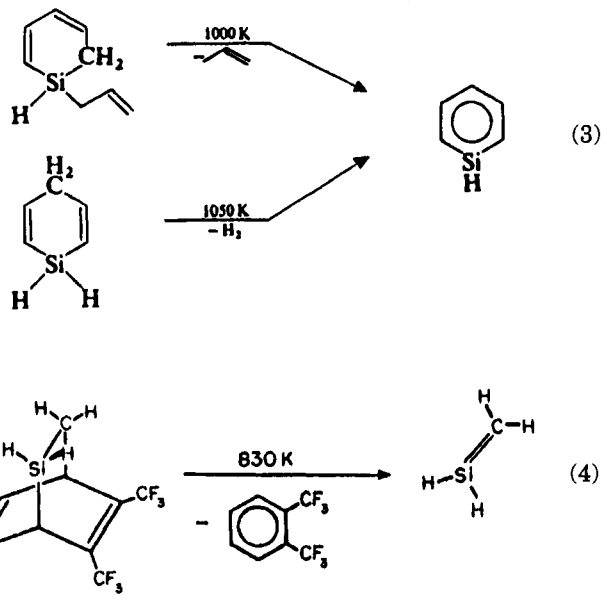

Other derivatives with Si=C[1d] or Si=Si[1e] double bonds, which are stabilized kinetically by bulky substituents, can be isolated and often their structure determined.[19]

Another valuable technique for investigation of short-lived intermediates is isolation in inert matrices at low temperatures:[19] The matrix photolysis of azidosilane H_3SiN_3 to HNSi + H_2 + N_2 reported in 1966,[13] and the extensive quantum-chemical calculations on the isomers HSiN ↔ HNSi,[23] which suggest that HN≡Si is the thermodynamically more stable by 237 kJ mol^{-1}, have been the starting point for our attempt to pyrolyze triazidophenylsilane at 10^{-4} mbar (Figure 9):[13]

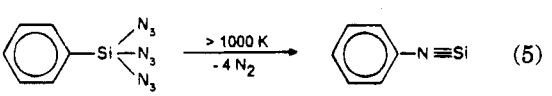

The "controlled explosions" of the triazidophenylsilane in a close to unimolecular flow system at low pressure can only be accomplished using a white-hot quartz tube, i.e. temperature in excess of 1000 K! As with other azides,[24] this can be carried out safely with small amounts of sample using PE spectroscopic real-time gas analysis.[7] Optimization of the N_2 extrusion conditions by inspection of the ionization patterns recorded with increasing temperature shows $H_5C_6Si(N_3)_3$ to be completely desomposed at 1100 K: its strong σ_{N_3}-ionization band[24] between 15 and 16 eV has been replaced by the intense N_2 ionization peaks (Figure 9, filled peaks).

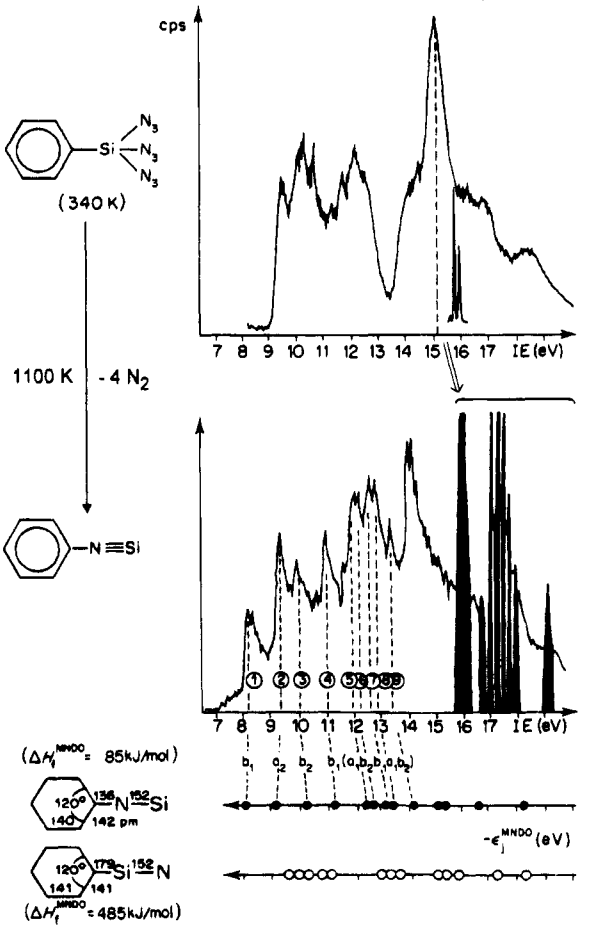

Figure 9. He I spectra of triazidophenylsilane at 340 K and its pyrolysis products at 1100 K (N_2 bands in black). The assignment of the 1100 K spectrum to one of the isomers $H_5C_6N{\equiv}Si$ or $H_5C_6Si{\equiv}N$ via Koopmans' correlation, $IE_n^v = -\epsilon_j^{MNDO}$, is based on the eigenvalues from geometry-optimized MNDO calculations (see the text).

In the low-energy region between 8 and 14 eV, the pyrolysis mixture exhibits an ionization pattern consisting of nine well-separated bands (Figure 9). These are assigned to phenyl silaisocyanide on the basis of comprehensive calculations via Koopmans' theorem, $-\epsilon_j^{SCF} = IE_n^v$.[1-3] In contrast, for the isomeric silacyanide $H_5C_6Si{\equiv}N$, only two ionization humps of strongly overlapping bands between 9.5 and 11 eV and around 13 eV are suggested (Figure 9, unfilled circles), which do not fit the observed PE spectroscopic pattern. Fully geometry-optimized MNDO calculations also predict $H_5C_6N{\equiv}Si$ to be more stable than $H_5C_6Si{\equiv}N$ by some 400 kJ/mol, paralleling the calculated total energies for the parent isomers HNSi and HSiN.[23] Furthermore, the optimized bond length $d_{N{\equiv}Si}^{MNDO}$ = 152 pm agrees well with the 154 pm determined by IR spectroscopy and from highly correlated calculations for HN≡Si.[13,23] For the pyrolysis product $H_5C_6N{\equiv}Si$, a linear arrangement of (C)N≡Si with a singly coordinated, triply bonded silicon is calculated.

In addition, the PE spectroscopic results have been further supported by the matrix isolation of phenyl silaisocyanide.[13] The two experiments complement each other and, therefore, provide overlapping evidence that the pyrolysis of triazidophenylsilane,

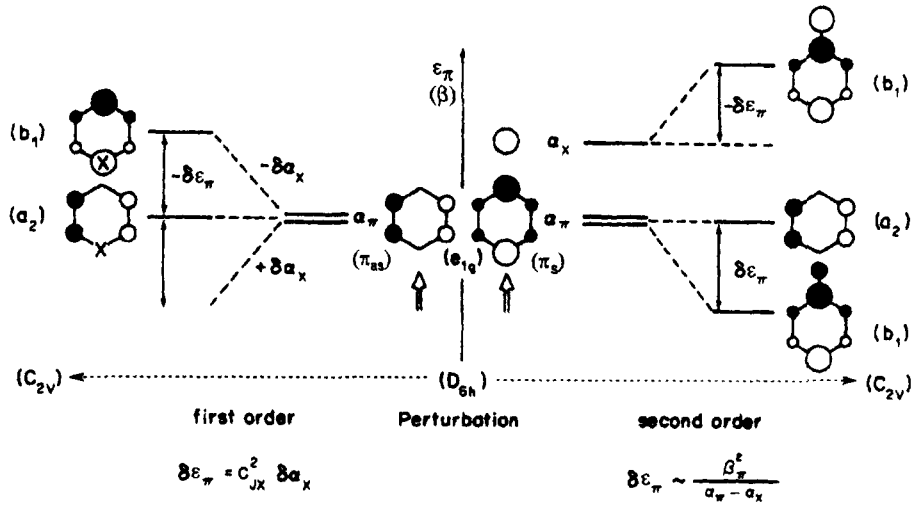

Figure 10. First- and second-order perturbations exemplified for benzene and its symmetry correct (open arrows) internal and external ring monosubstitution from D_{6h} to C_{2v}, which lifts inter alia the degeneracy of the $\pi(e_{1g})$ molecular orbitals. Within first-order ring center exchange C → X, only the orbital π_s with no nodal plane through the substituted center is lowered by electron donors X($-\delta\epsilon_\pi$) and raised by electron acceptors X($+\delta\epsilon_\pi$). For skeleton extensions by an additional external center X within second-order perturbation, the molecular orbitals of the same symmetry representation are "mixed" and, therefore, lowered ($+\delta\epsilon_\pi$) by additional bonding (○−○) interaction and raised ($-\delta\epsilon_\pi$) by a corresponding antibonding (○−●) one. First-order perturbations $\delta\alpha$ are proportional to the square of the coefficient ($c_{\pi\mu}$) of the perturbed center μ, while second-order perturbations increase with the squared interaction parameter (β^2) as well as with the decreasing energy difference ($\Delta\alpha$) between the starting levels.

Chart 1

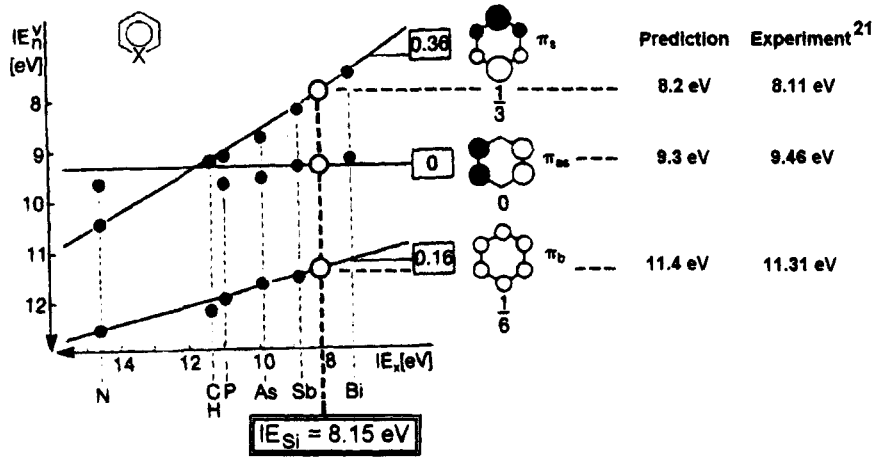

(6)

driven by the energetically favorable extrusion of four molecules of N_2, enforces, under the unimolecular conditions applied, the formation of the first, and still unique, organosilicon molecule with a terminal silicon of coordination number 1 within a N≡Si triple bond.

4. First- and Second-Order Silicon Substituent Perturbations

For the interpretation of molecular state measurements (Figures 1 and 2), a comparison of data for chemically related compounds is extremely valuable, especially those for differently substituted parent π systems based on first- and second-order perturbation arguments (Figure 10).[1-3]

Among the numerous rationalizations of radical cation state data by first-order perturbation (Figure 10), an especially impressing one has been the correct prediction[3] of the three lowest vertical ionization energies of silabenzene, which was generated and characterized by PE spectroscopy (3) only 2 years later.[21] The starting point was a known[25] correlation between the PE spectroscopically determined vertical π-ionization energies of benzene and its monohetero derivatives $(HC)_5XR$ and the ionization energies ($^4S_{3/2} \rightarrow {}^3P_0$) of the perturbing atoms X, in which the gradients of the resulting regression lines (Chart 1, values in boxes) reflect the squared coefficients, ($c_{\pi\mu}^2$) of the perturbed center μ (Figure 10).

On insertion of the silicon atom ionization energy of 8.15 eV, correct approximate predictions of the π-ionization energies of the then still unknown silabenzene[3] resulted (Chart 1, unfilled circles), which helped considerably in optimizing the thermolysis conditions for its first generation in a newly designed short path flow system under nearly unimolecular conditions[1,2,20,21] by PE spectroscopic real-time gas analysis.[7]

The most clear-cut example of second-order perturbation orbital mixing (Figure 10) in organosilicon radical cation states is provided by silylacetylene. (**Caution**: explosive mixtures with air!) The electron distribution can be formally subdivided into a

cylindrical electron cloud around the CC bond and the C_{3v}-symmetric "three-bladed H_3Si propeller". The "hyperconjugative" interaction in $H_3SiC{\equiv}CH^{\bullet+}$ between the two ^2E radical cation states of identical symmetry can be determined by calibration with the ionization energies $IE_1^v = \alpha_{CC}$ to $HC{\equiv}CH^{\bullet+}$ and the mean value $\overline{IE_{2-5}}(SiH_3) = \alpha_{SiH3}$ for the Jahn/Teller-distorted $H_3SiSiH_3^{\bullet+}$ (Figure 4) as suggested by the photoelectron spectrum and the obvious splitting scheme:[26]

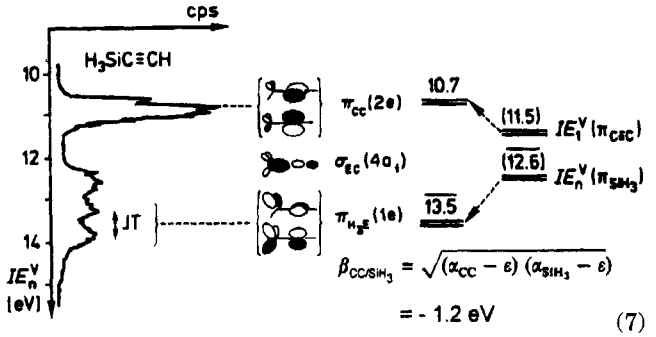

(7)

Inserting the respective ionization energies into the second-order interaction determinant (7) yields the parameter

$$\beta_{CC/SiH_3} = \sqrt{(IE_1(HC{\equiv}CH) - IE_1)(IE_n(SiH_3) - IE_1)}$$
$$= \sqrt{(11.05 - 10.7)(12.6 - 10.7)}$$
$$= (-)1.2 \text{ eV}$$

which on comparison with the interaction parameter $\beta_{CC/CH_3} = -2.1$ eV for methylacetylene[26] confirms that the hyperconjugation π_{CC}/σ_{CH_3}, is even more effective, as expected from the shorter bond length $C{-}C(H_3)$ and the resulting increased overlap.[26] Hyperconjugation radical cation state models (7) are widely applicable and include, inter alia, doubly substituted disilylacetylene, $H_3SiC{\equiv}CSiH_3$, or silicon halides, H_3SiHal.[1,2]

ESR/ENDOR spectroscopic nuclear hyperfine coupling constants (cf. section II.2) of organosilicon radical cations generated in solution (Figure 7), provide interesting information on the distribution of the unpaired electron over the molecular skeleton[16] (cf. Figure 8 and (2)). In $(R_3Si)_nCH_{3-n}$-substituted cations, the spin population ϱ^π is transferred by angle-dependent "σ/π-hyperconjugation". The coupling constants a_X are best rationalized by the Heller/McConnell equation,[8,16] $a_X = (B_o + B_2 \cos^2 \Theta_{CX})\varrho_\mu^\pi$. All constants B_o^H, B_o^{Si}, and B_2^H, B_2^{Si} are accessible from correlations of $\alpha_{H,Si}$ vs $\cos^2 \Theta_{CX}$ within series of radical cations with preferred conformations such as those shown in Chart 2.[1,2,16]

The conformational assignments from the ESR/ENDOR spectra can be further substantiated by a simplified first-order perturbation model for their vertical first-ionization energies using the same angular increments ($\cos^2 \Theta_{CX}$):[1,2,27] Parametrization for toluene and its 3-fold R_3Si-substituted derivative ($1 \times \cos^2 0° + 2 \times \cos^2 60° = 1.5$) and for the corresponding xylenes ($\Sigma\langle\cos^2 \Theta\rangle = 3.0$) yields $d_{CH} = 0.27$ eV and $d_{CSi} = 0.68$ eV as average "hyperconjugation" values. On insertion into the perturbation formula, $IE_1^v = \Sigma d_{CX}\langle\cos^2 \Theta\rangle$, a good reproduction of the experimental data is achieved. For the mono- and disubstituted benzene derivatives $R_3SiH_2CC_6H_5$ and $1,4\text{-}R_3SiH_2CC_6H_4CH_2SiR_3$, for instance, the PE spectroscopically determined first vertical ionization energies, $IE^v = 8.35$ and 7.75 eV, are satisfactorily predicted to be 8.43 and 7.60 eV.[1,27] To rationalize the procedure within the general first-order perturbation approach (Figure 10), the parameter $\delta\alpha_X$ has been replaced by the angle-dependent bond increment, $d_{CX}\langle\cos^2 \Theta_X\rangle$, which allows both spin transfer and electron ionization to be included.

In closing this essential subsection, which attempts to sketch out the importance of molecular state data correlation within series of chemically related compounds based on various perturbation approaches (Figure 10), two more facets need to be emphasized.

The first concerns the size effects in larger molecules such as are obvious in the 4-fold $(H_3C)_3SiCH_2$-substituted ethene and benzene derivatives, $C_{18}H_{44}Si_4$ and $C_{22}H_{46}Si_4$. They exhibit almost identical first vertical ionization energies and, therefore, the two very different π subunits, ethene and benzene, seem to lose their identity:[1-3]

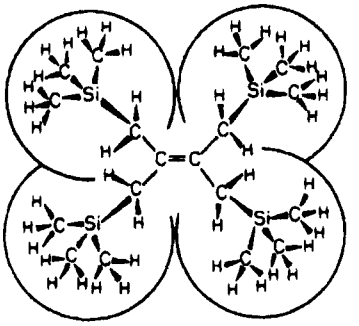

(8)

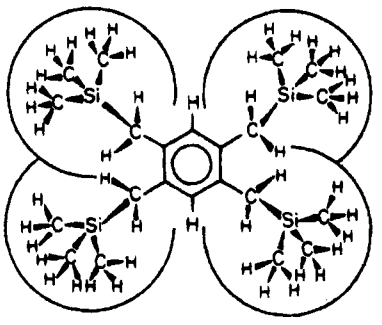

The spin and charge delocalization observed in organosilicon radical cations and the additional information from the structures of sterically overcrowded molecules[4] allow an easy explanation that both of the above molecules are tetrahedrally shaped (8) each with two R_3SiCH_2 groups above and below the central skeletal plane. Accordingly, the positive hole generated by electron expulsion must be distributed in an analogous way within their hydrocarbon skins.[1-3]

Secondly, more general remarks referring to the molecular state model (1) introduced at the very beginning and its properties are directed to the topological connection between the individual centers within molecules, their overall symmetry, their effective nuclear potentials, and the resulting electron

Chart 2

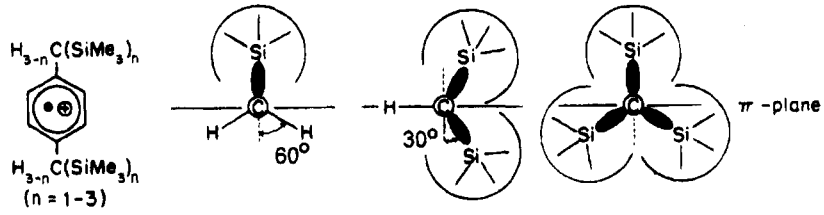

(9)

distribution.[3] Many more criteria are available for informative correlation of experimental data such as coordination numbers of essential centers, the connection of the individual subunits and their spatial arrangement especially in isoconjugate systems or for heteroconjugate systems, the different framework potentials, and the respective number of valence electrons. The tremendous achievements in both hardware and software for quantum-chemical calculations have provided indispensable help in understanding molecular states within the general approach (1). This will be elaborated on within the last introductory subsection presented here.

5. Semiempirical Calculations for Si-Containing Molecules

Within the period covered by this review, 1988 to 1994, the progress of numerical quantum chemistry has been overwhelming. Referring to more authoritative reviews by professional theoreticians, the application-minded chemist has witnessed the development from medium-sized, main-frame computers to fast, readily accessible workstations and the improvement in ab initio methods including Moeller/Plesset perturbation correlation as well as the rebirth of an old method, density functional calculations, to an effective and fashionable tool. Understandably, the following remarks will be confined to semiempirical approaches such as the already outdated CNDO or INDO and increasingly old-fashioned methods such as MNDO,[28] AM1,[29] or PM3.[30] Nevertheless, all of these have been effective and valuable over many years to silicon chemists, who in general have been satisfied with the parametrization[31] offered for most of their organosilicon compounds.

An illustrative example, typical for organosilicon radical cation investigation in solution and which provided unexpected, puzzle-solving, and, therefore, extremely helpful answers at the time, when any information concerning both energy as well as spin distribution was otherwise inaccessible, is the oxidation of silyl-substituted hydrazine derivatives by the oxygen-free and selective one-electron-transfer reagent $AlCl_3/CH_2Cl_2$[16,17] (Figure 7). One of the cornerstone results has been the satisfactory simulation of the high-resolution ESR spectrum including the ^{29}Si coupling (Figure 8) of the planar 1,5-diaza-2,4,6,8-tetrasilabicyclo[3.3.0]octane derivative in its paramagnetic doublet ground state:

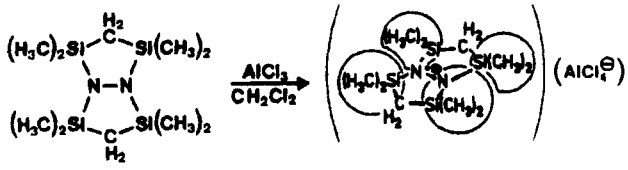

(10)

Problems, however, resulted on comparison with the analogous silyl hydrazine radical cations such as the branched chained $((H_3C)_3Si)_2N^{\bullet+}N(Si(CH_3)_3)_2$, for which the obvious different angular dependence of the dominant couplings a_N and a_H remained an unsolved question. INDO open shell hypersurface calculations[9] for the parent compound $H_2N\text{-}NH_2^{\bullet+}$,[16] in which all degrees of freedom for the $3N - 6 = 12$ dimensional problem could be considered by choosing the three possible angles α(HNH), β(NNH), and ω-(H_2NNH_2),[9] yielded all the information needed (Figure 11): Upon one-electron removal, $H_2NNH_2 \rightarrow H_2NNH_2^{\bullet+} + (e^-)$, the 87° twisted neutral parent compound with a 145 pm long N–N single bond becomes planar, going from C_2 to D_{2h} symmetry. The $N{=}N^{\bullet+}$ bond shortens by 17 pm to 128 pm! The calculated a_N and a_H coupling hypersurfaces predict different angular dependence, with a_N exhibiting a single minimum at $\omega(H_2NNH_2^{\bullet+}) = 90°$ and a_H two minima at about 60° and 120°.

All the facets revealed by the approximate INDO open shell hypersurface calculations for the model radical cation $H_2NNH_2^{\bullet+}$, especially the predicted drastic structural changes $C_2 \rightarrow D_{2h}$, including the formation of a two-center/three-electron multiple bond $N{=}N^{\bullet+}$ and the differing angular dependence of the a_N and a_H coupling constants, have been confirmed. A tetraalkylated hydrazine radical cation salt, $[(H_2C)_6(HC)_2N{=}N(CH)_2(CH_2)_6^{\bullet+}][PF_6^-]$, was crystallized a year later and its structure determination demonstrated a 127 pm long $N{=}N^{\bullet+}$ bond[32] close to the approximate estimate of 128 pm (Figure 11). The a_N/a_H diversity has been detected, e.g. also for boron-substituted hydrazine radical cations.[33]

There have been numerous other successes of semiempirical calculations, for example, the PE spectroscopic assignment for the novel molecule $H_5C_6N{\equiv}Si$ with a singly coordinate, triply bonded silicon and the comparison with the isomer H_5C_6-$Si{\equiv}N$ and its MNDO-predicted ionization pattern, structure, and enthalpy of formation (Figure 9). Except for small conformational changes, the semiempirical calculations reproduced most experimental data almost numerically correctly. Bond lengths were determined to within ±3 pm and angles usually to better than ±3°. The unavoidable Koopmans' deviations, $D = IE_n^V - \epsilon_j^{SCF}$, of eigenvalue sequences rarely exceeded 0.5–1 eV, depending on molecular size and moderate effective nuclear charges for most centers. In general, semiempirical calculations by various procedures were essential for the discussion and the understanding of the organosilicon radical cation states.[1,2]

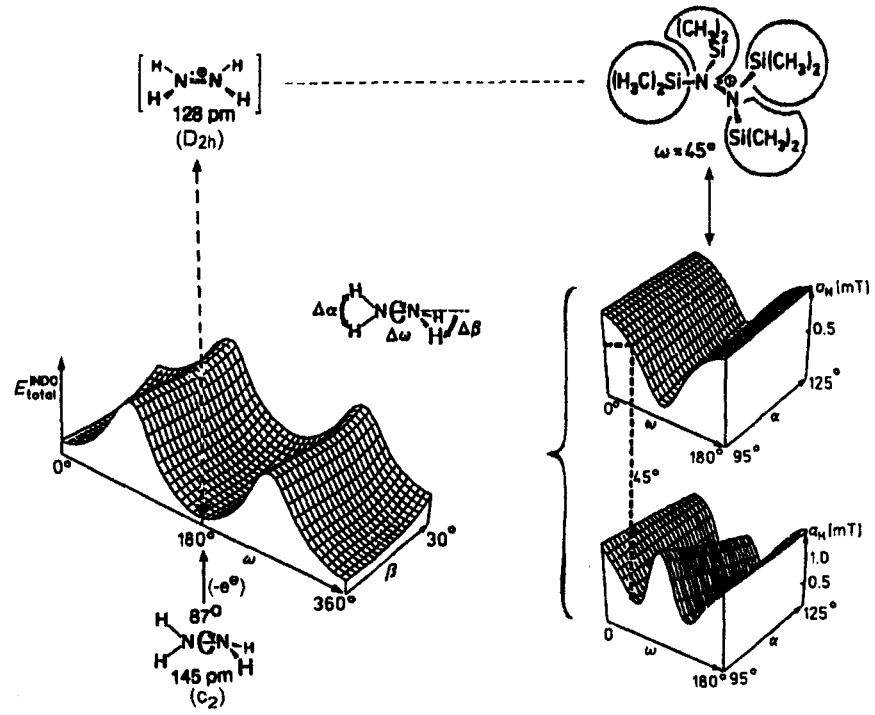

Figure 11. INDO open shell hypersurfaces both for the total energy and the structure of the radical cation $H_2NNH_2^{\bullet+}$ as well as for the angular dependence of the coupling constants a_N and a_H including a structural estimate for the sterically overcrowded tetrakis(trimethylsilyl)hydrazine radical cation in solution (cf. the text).

III. Recent Photoelectron Spectroscopic Investigations

The preceding introductory "classical" examples were intendend to provide the minimum necessary basics[1-3] for a discussion of more recent research results for organosilicon radical cations both in the gas phase and in solution (sections III and IV). Methods of generation of ions by single electron ionization in the gas phase under nearly unimolecular conditions or by one-electron oxidation in aprotic inert solvents (sections II.1. and II.2), instrumental techniques to investigate their various molecular states such as photoelectron as well as ESR/ENDOR spectroscopy (sections II.1−3), principles to compare equivalent $M^{\bullet+}$ states of chemically related molecules M such as first- and second-order perturbation (section II.4), and the much appreciated help of quantum chemistry to solve numerous experimental problems (section II.5) have been presented. In addition, a most valuable and basically qualitative approach to structure ↔ energy relationships in molecular states (1) has been proposed, specifying the topological connections and symmetry aspects in detail. In conclusion, all PE spectra reported since the publication of the previous reviews[1,2] are compiled and commented upon.

1. Silylenes

Silylenes SiX_2 are an interesting class of molecules with doubly coordinated silicon.[1,2] They are attractive from theoretical,[34] spectroscopic,[1,35,36] preparative,[19] and industrial[37] points of view. Highlights are selected from the vast literature: The parent molecule SiH_2 has a singlet ground state $X(^1A_1)$ in contrast to the triplet $X(^3B_1)$ of the isoelectronic carbene.[34] Some organosilylenes are colored;[19] even $(H_3C)_2Si$ is yellow. Derivatives with bulky substituents R dimerize to disilanes, $2R_2Si \rightarrow R_2Si{=}SiR_2$.[19] H_3CSiCl is presumably the intermediate in the Rochow/Müller process for methylchlorosilanes.[37] Gas-phase structures have been determined for $SiCl_2$ and for $SiBr_2$ by electron diffraction.[1]

The PE spectroscopic studies of silylenes, confined so far to the dihalogen derivatives SiX_2, with X = F, Cl, and Br[1,18,35] (Figure 12), have now been extended to the kinetically unstable SiI_2 (Figure 12) and to the surprisingly stable five-membered ring derivative $(HC)_2(NC(CH_3)_2)_2Si$ (Figure 13). In addition, H_3CSiH has been investigated by Fourier transform ion cyclotron resonance spectroscopy.[38]

The SiI_2 story concerns a novel triatomic molecule with a relativistic touch and begins with a topological exercise (1) based on combinatorics:[35] The 13 most important nonmetal elements (H, B, C, Si, N, P, O, S, F, Cl, Br, I, Xe) allow the construction of 1638 triatomic molecules, of which 1183 are linear and 455 are cyclic. A literature search demonstrates that most of them have already been reported, but that the monomer SiI_2 is one of the few exceptions and, therefore, became the first triatomic molecule discovered by the Frankfurt PES group! Its preparation[35] in a short path gas flow system by passing SiI_4 over heated silicon $[Si]_x$ is analogous to that for $SiCl_2$ and $SiBr_2$ (Figure 12).

For the assignment of the radical cation state, it is advantageous to start with the less relativistically dominated $SiBr_2$, for which MNDO diagrams are presented (Figure 12, bottom). These predict the following plausible sequence[35] for the seven lowest ionizations within the He I measurement region, which are expected from the altogether 12 $3p_{Si}$ and $4p_{Br}$ and the two $3s_{Si}$ valence shell electrons. The $M^{\bullet+}$ ground state $X(^2A_1)$ is generated by electron expulsion

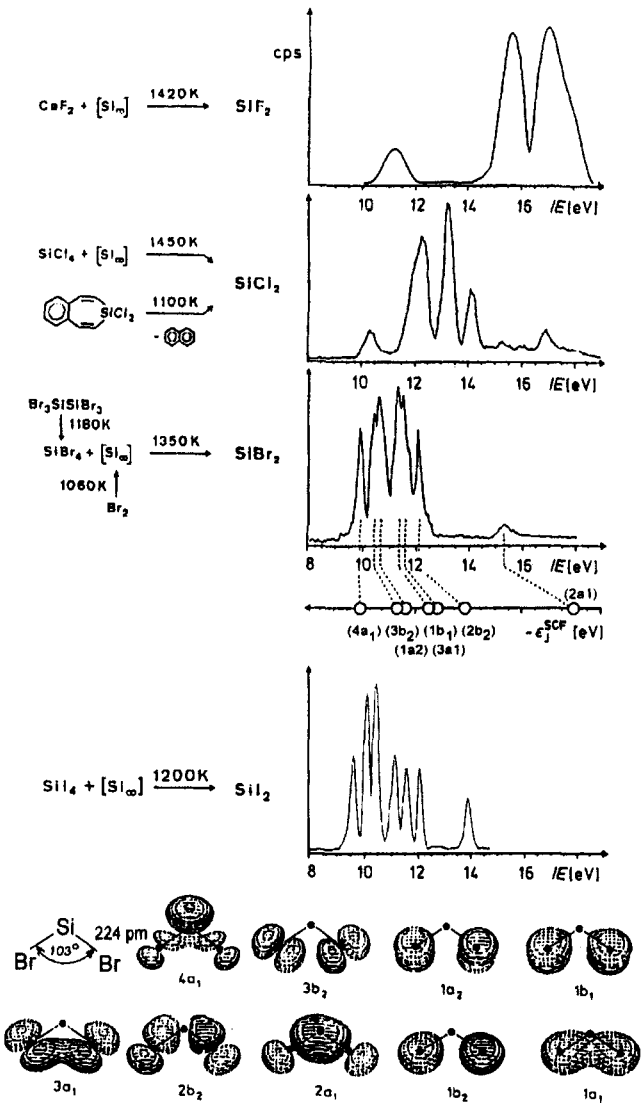

Figure 12. Preparation and PE spectroscopic characterization of SiF_2, $SiCl_2$, $SiBr_2$, and SiI_2, with Koopmans' assignment of the radical cation states of $SiBr_2$, based on MNDO eigenvalues and eigenfunctions calculated without spin/orbit coupling (cf. text).

from the silicon electron pair ($4a_1$), followed by four n_{Br} bromine electron pairs (Figure 12, $3b_2$, $1a_2$, and $3a_1$) and two σ_{SiBr} ionizations ($2b_2$ and $2a_1$), the latter with a dominant $3s_{Si}$ contribution. On comparison of PE spectra of SiF_2, $SiCl_2$, and $SiBr_2$ (Figure 12), the lowering of the halogen electron pair ionization $n_F > n_{Cl} > n_{Br}$ catches the eye. The effect reflects the tremendous influence of the decreasing effective nuclear charge of the halogen substituents.[39] For SiI_2, its different ionization band pattern (Figure 12) already suggests that relativistic effects can no longer be neglected. According to relativistic Dirac–Fock calculations, the 5s and $5p_{1/2}$ orbitals are contracted by 3.9 and 4.0%, whereas the $5p_{3/2}$ expands slightly by 0.6%. Energetically, the 5s and $5p_{1/2}$ orbitals are stabilized by 1.52 and 0.7 eV, whereas the $5p_{3/2}$ orbital is destabilized by 0.39 eV. Experimentally, hyperfine splittings of the ($5s^2$, $5p^5$) states are determined to be 0.94 eV for the iodine atom and 0.67 eV for $HI^{\bullet+}$.[39] Relativistic two-component pseudopotential SCF calculations with a double ζ polarization function basis set[35] satisfactorily reproduce the ionization sequence observed by PE spectroscopy for SiBr; the largest Koopmans' deviation amounts to only 0.33 eV. The spin/orbit coupling effects are calculated to be negligibly small.[35] The optimized structural parameters of $d_{SiI} = 250$ pm and $\angle ISiI = 103°$ as well as the charges of Si +0.54 and I −0.27 fit nicely into the dihalogen silylene series (Figure 12), which is dominated by the decreasing effective nuclear charges of the halogen substituents.[39]

The other silylene story, published in 1994, is also breathtaking: Following the surprising discovery of the first "bottlable" carbenes by Arduengo and collaborators[40] as well as of the subsequent analogous germanium derivatives,[41] the first isoelectronic silylene has been synthesized and crystallized and its structure determined.[42]

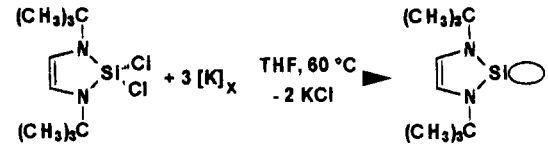

(11)

The photoelectron spectrum[36] (Figure 13) is best discussed by radical cation state comparison with the isosteric C and Ge derivatives and, as emphasized, based on the results of density functional calculations with a triple-ζ basis set (e.g., Si, 73111/6111/1).

The comparison of the radical cation states of the three isosteric molecules $(HC)_2(NC(CH_3)_3)_2X$ with X = C, Si, or Ge reveals (Figure 13) that the ground state of the carbene $\tilde{X}(^2A_1)$ is dominated by an n_C lone pair contribution, whereas both the silylene and the germylene exhibit π-type states, $\tilde{X}(^2B_1)$. According to the density functional calculations, the crossover $n_C/\pi_1 \rightarrow \pi_1/n_{Si}$ (Figure 13, 7.68 → 8.21 eV and 8.22 → 6.96 eV) can be readily rationalized by the calculated densities, viewed both in the molecular plane (Chart 3, part A) and in the plane bisecting the C=C double bond and the two-coordinate main group element (Chart 3, part B).

In close-to-perfect agreement with the experimentally determined electron distribution in 1,3,4,5-tetramethylimidazol-2-ylidene-d_{12},[36] around the divalent C center an ellipsoidally distorted n_C lone pair density is calculated, whereas the distribution at both the Si and the Ge centers[36] is essentially spherical. Therefore, although the decrease in effective nuclear charge C << Si < Ge shows a considerable decrease in the π_1 ionization energies (Figure 13; C, 8.22 → Si, 6.96 → Ge, 66.5 eV) there is a smaller charge, $\Delta IE_3{}^v = 9.24-8.80 = 0.44$ eV, for the π_2 ionization.[36] The ionization energies of the lone pair increases in the opposite direction, $n_C \rightarrow n_{Si}$, as can be rationalized by their varying electron density shape from ellipsoidal n_C to circular n_{Si}.[43]

Further literature without direct relevance to experimental investigations on organosilicon radical cation states, such as results of collisional activation and neutralization–reionization mass spectroscopy on $(H_3C)_2Si^{\bullet+}$ [44] or $H_2SiCO^{\bullet+}$,[45] reaction products from $Si^+ + R_nSiH_{3-n}$,[45] the detection of $SiCl^{\bullet}$ by resonance-enhanced multiphoton ionization spectroscopy,[47] or calculations for $SiH_2^{\bullet+}$ [48] or $SiX_2^{\bullet+}$,[49] are not presented in detail.

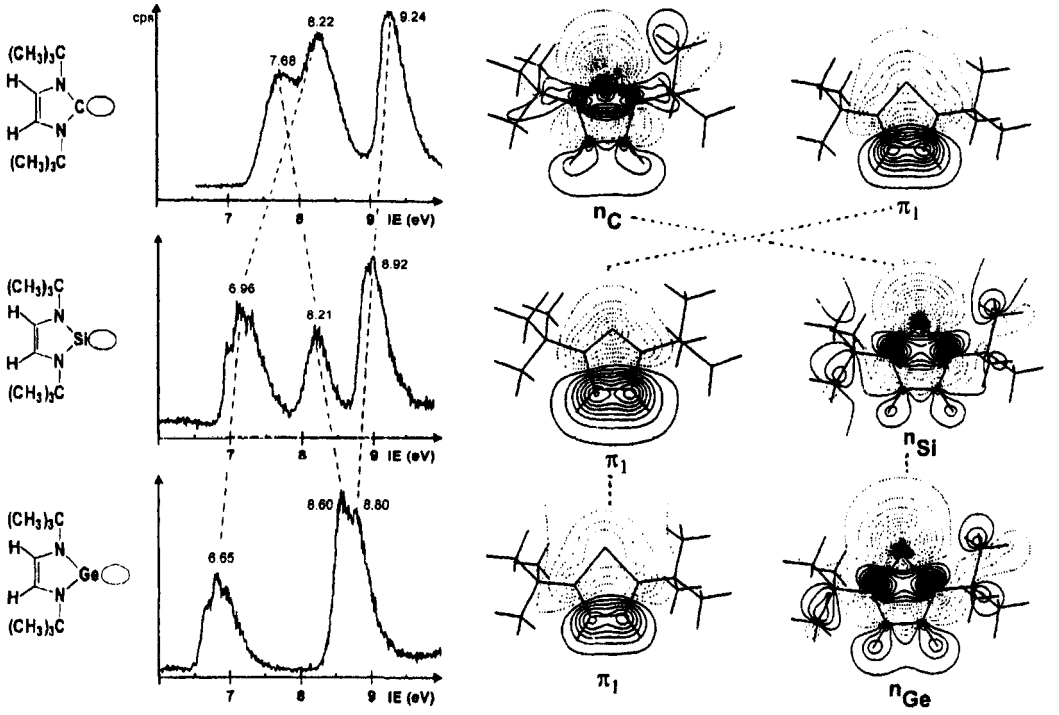

Figure 13. High-resolution photoelectron spectra in the 6–10 eV region of the carbene (1,3-di-*tert*-butylimidazol-2-ylidene), the silylene (1,3-di-*tert*-butyl-1,3,2-diazasilol-2-ylidene), and the analogous germylene (1,3-di-*tert*-butyl-1,3,2-diazagermol-2-ylidene), with assignment of the first two $M^{\bullet+}$ states by density functional molecular orbitals n_X and π_1 (cf. the text).

Chart 3

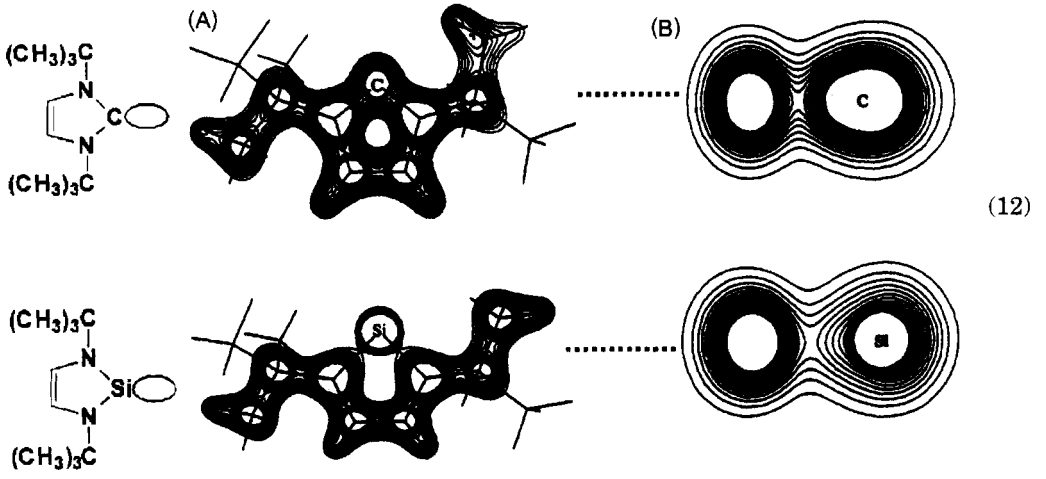

2. Siloxanes and Silathianes

Lone pair n_x vertical ionization of saturated molecules with heteroatom centers often generate their radical cation in the ground state (Figure 1) and, therefore, are well-suited to probe substituent effects.[1,2] Within the review period 1989 to 1995, organosilicon oxygen[50] and sulfur[51–54] derivatives have been investigated by photoelectron spectroscopy with special emphasis on the sometimes tremendous donor properties of of groups $CH_{3-n}(SiR_3)_n$.[1,2,18]

Starting with the organosilicon sulfur derivatives (Figure 14), the first vertical "sulfur π lone pair" ionizations of the molecules ranging from the parent triatomic H_2S through saturated sulfides with alkyl and silyl substituents span a wide range of 2.8 eV down to $((H_3C)Si)_3CSCH_3$, with its "Guiness book of records" low IE_1^v = 7.66 eV.[51] The substituent effects, which increase in the order H < SiH_3 < $Si(CH_3)_3$ ~ CH_3 < $CH_2Si(CH_3)_3$ < $C(Si(CH_3)_3)_3$, are mostly nonadditive: For instance, within the series of β-[(trimethylsilyl)methyl] derivatives $SH_{2-n}(CH_2SiR_3)_n$ the differences between n = 0, 1 and n = 1, 2 are 10.47–8.96 = 1.51 and 8.96–8.03 = 0.93 eV[51] (Figure 14). For rationalization, orbital pertubation models (section II.4) are unsatisfactory, due to both the large size of many compounds and their low symmetry. With respect to the equivalent radical cation ground states of the chemically related sulfide molecules, however, and the fact[6] that vertical electron expulsion, $M \rightarrow M^{\bullet+} + e^-$, occurs within 10^{-15} s, i.e. a period orders of magnitude before vibrations start to change the "frozen" M ground state structure to the optimal state for $M^{\bullet+}$ stabilized by charge delocalization, the preceding molecule-specific "electronic relaxations" must be essential in the ionization process. For this reason, the charge distributions around the sulfur centers in the neutral sulfides have been calculated and correlated with the respective

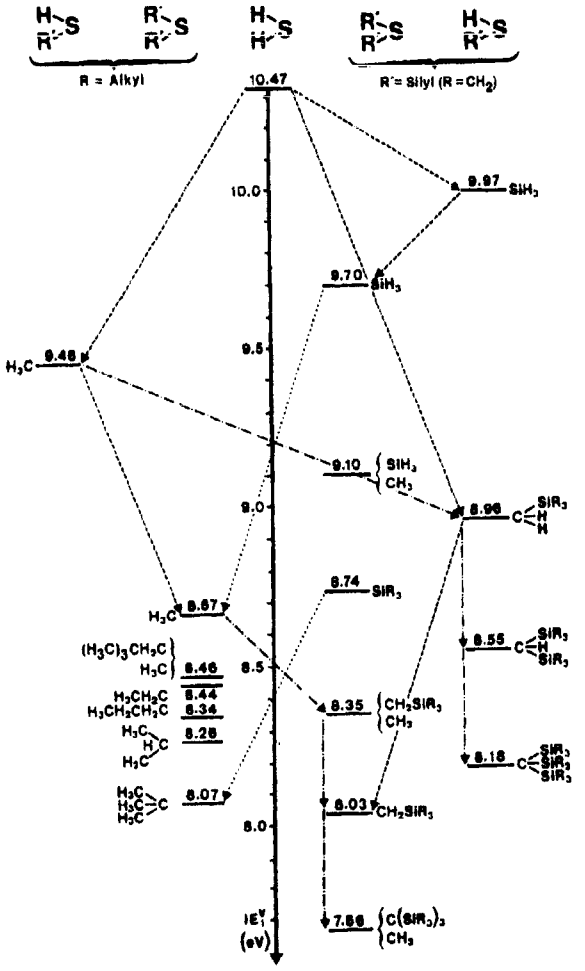

Figure 14. First vertical ionization energies $IE_1^v(n_S)$ (eV) of H_2S and its alkyl, silyl, trimethyl and (trimethylsilyl)-methyl derivatives: (– –) identical mono- and disubstitution, (• •) alkyl/silyl comparison, (– • –) β-silyl substituent effects.

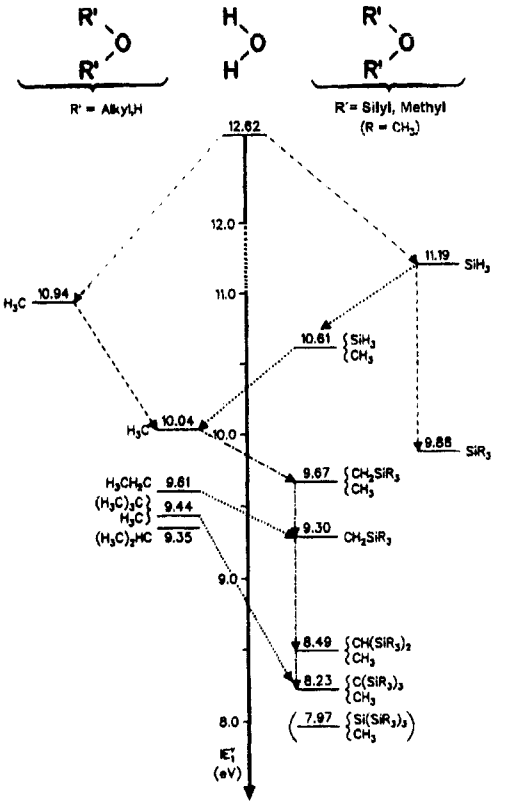

Figure 15. First vertical ionization energies $IE_1^v(n_O)$ (eV) of H_2O and its alkyl, silyl, trimethyl, and (trimethylsilyl)-methyl derivatives: (– –) identical mono- and disubstitution, (• •) alkyl/silyl comparison, and (– • –) β-silyl substituent effects.

first vertical ionization energies, as seen in Chart 4.[50]

Obviously, this approach, which neglects all other aspects of the complex ionization process and does not account specifically for the change in correlation energies between M and $M^{\bullet+}$, nevertheless yields a satisfactory linear regression and thus provides some indication that the charge delocalization in the radical cations generated vertically in the "frozen" struture of the neutral molecules, i.e. to their electronic relaxation before the onset of vibration, is an essential feature in the ionization process of organosilicon sulfides,[51–53] a point of view not covered by orbital interaction models.[54]

The siloxane derivatives (Figure 15) show additional features. The perturbation of the lone pair

Chart 4

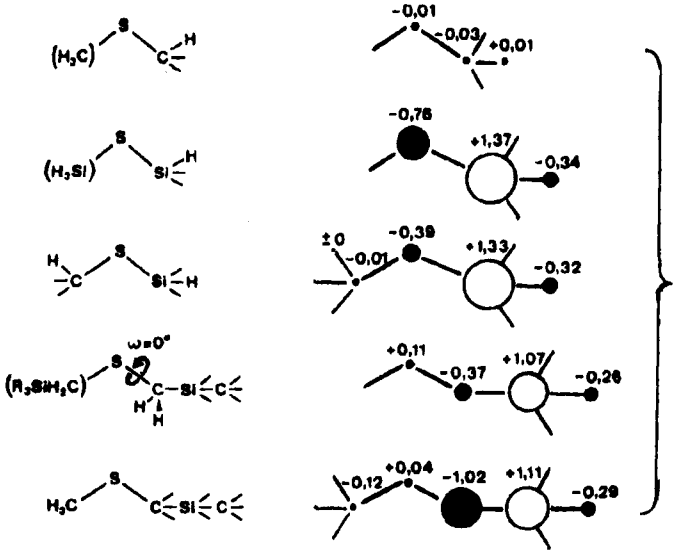

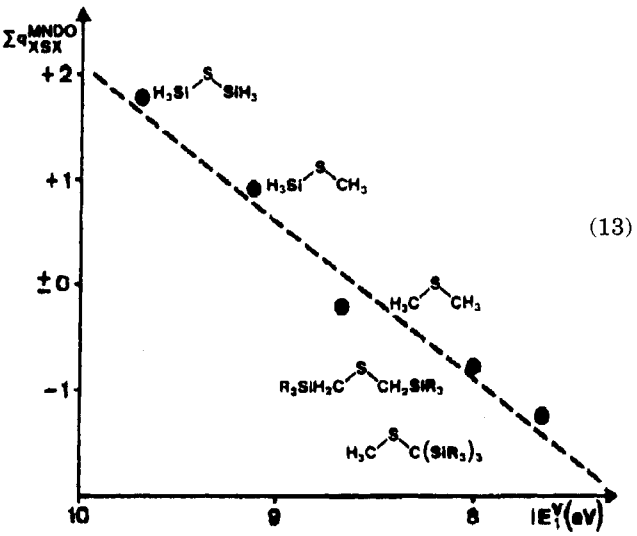

(13)

by the β-silyl group is greater in the oxides than in sulfides:[52]

	IE^v_1(eV)	R = H	$Si(CH_3)_3$	ΔIE^v_1(eV)
X = O		10.57	9.07	1.50
S		9.03	8.19	0.84

(14)

For rationalization, the very different effective nuclear charges, $Z_{eff}(O) >> Z_{eff}(S)$,[2] as well as the much shorter bond lengths of ~142 pm for CO vs ~182 pm of CS[55] are dominant factors. Consequently, the differences in vertical first-ionization energies range from 12.62 eV for H_2O over 4.7 eV to 7.92 eV for $H_3CSC(Si(CH_3)_3)_3$ (Figure 14), a difference of almost 170%! The β-silyl pertubation of n_O lone pairs is one of the largest substituent effects ever detected by PE spectroscopy.[1-3,15] Again no additive increments are found for β-silyl groups, as is convincingly demonstrated by the ionization energies IE_1^v for isomers such as those shown below.[50]

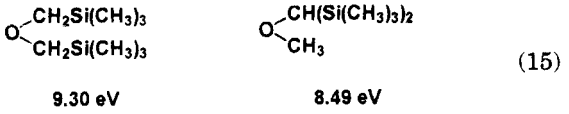

IE_1^v	9.30 eV	8.49 eV

(15)

Due to steric overcrowding in the organosilicon oxygen derivatives, which is increased due to the shorter OC bonds relative to that in the respective sulfides, the simple correlation of $IE_1^v(n_S)$ vs the sum Σq_{XSX}^{MNDO} of calculated charges around the ionized S center has to be extended to an angle-dependent model such as that introduced as a classic example (Chart 2). The total perturbation, P, for example $H_3COC(Si(CH_3)_3)_3^+$, may be calculated from the geometry-optimized semiempirical structures, calibrated by the measured IE_1^v (eV) values, and includes for the difference $\Delta Z_{eff}(O/Si)$ additive, angle-independent increments. Using the calculated values, the first vertical ionization energy is reproduced satisfactorily in Chart 5.

Additional cyclovoltammetric measurements yielded (irreversible) oxidation potentials E^{Ox} between +1.54 and +1.87 V, which nevertheless can be linearly correlated to the first ionization potentials, E^{Ox} (V) = $-0.576 + 0.259IE_1^v$ (eV) with $R = 0.985$.[50]

Other publications on gas phase investigations of β-silyl-substituted oxygen and sulfide radical cations either neglect known facts,[1,16] and therefore, base their arguments on misleading assumptions,[56] present calculations for silicon oxygen hydrides $Si(OH)_{1-4}$[57] or focus on n_N lone pair containing organosilicon nitrogen derivatives, which are reported in section III.5.

3. Compounds with Bulky Organosilicon Substituents

Continuing with heterosubstituted organosilicon radical cations, the bis- and tetrakis(trimethylsilyl)-*p*-phenylene diamines[57,58] provide an interesting example for steric overcrowding. Single crystal structures have been determined by X-ray diffraction and the gas phase conformations investigated by photoelectron spectroscopy.[57] The starting point was the "Wurster's Blue" radical cation, discovered in 1879 and thoroughly investigated since then. The structures for both the *N,N,N',N'*-tetraalkyl-*p*-phenylene diamine precursors and their isolated redox-salts (Chart 6), exhibit a molecular skeleton in which the pyramidal N centers of the $(H_3C)_2N$ groups are completely flattened.

Surprisingly, the tetrakis(trimethylsilyl)-substituted *p*-phenylendiamine can be reduced to a "Wurster's Blue" radical anion as demonstrated by the observed benzene ring hydrogen quintet and the ^{29}Si silicon satellites in the ESR spectrum (section II.2). This seemingly strange attempt to reduce an already electron-rich molecule was stimulated by the assumption that due to H/H repulsion between the bulky $(H_3C)_3Si$ substituents with their van der Waals radius of 380 pm[4] and the adjacent ortho ring hydrogens, the $[(H_3C)_3Si]_2N$ groups should be twisted around the NC ring bond. The electron-donating n_N/π delocalization is replaced by Si → N electron withdrawal due to the huge difference in the effective nuclear charges, Si << N.[2] In 1994 we succeeded in proving the validity of this argument both for the solid neutral molecule by single crystal structure determination[57] as well as for the gas phase by quantum chemical analysis of the photoelectron-spectroscopic ionization pattern[57] (Figure 16). The optimized gas phase structure most likely applies for solution in aprotic solvents.

The structure-determining influence of the trimethylsilyl groups is clearly visible (Figure 16, AM1 geometry-optimized structural diagrams and space-filling representations of the X-ray analyses[57]): In the *N,N'*-disubstituted *p*-phenylenediamine, the n_N lone pairs of the planar $(R_3Si)HN$ subunits are coaxial with the π-vector perpendicular to the six-membered ring. In the tetrasubstituted derivative, the p-type N electron pairs of the also planar $(R_3Si)_2N$ subunits are twisted into the benzene plane due to the spatial overlap of the bulky $(H_3C)_3Si$ groups with the ortho ring hydrogens. The lack of n_N/π delocalization lengthens the NC bond from 141 to 144 pm[57] (Figure 16, structural diagrams, experimental values in brackets). The structure-determining interplay of counteracting n_N/π stabilization and H/H repulsion between the bulky $(H_3C)_3Si$ groups and the adjacent ring ortho hydrogens becomes especially apparent in

Chart 5

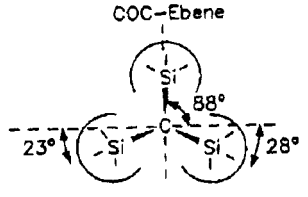

P_{total} = 10.04 eV − IE_1^v = $\Sigma\, \sigma_{SiC} \langle\cos^2\Theta\rangle + n \cdot 0.37$ eV

= 0.48 eV ($\cos^2 23° + \cos^2 28° + \cos^2 88°$) + 3·0.37 eV

= 1.89 eV

IE_1^v (calc.) = 10.04 eV − 1.89 eV = 8.15 eV

IE_1^v (exp.) = 8.20 eV

(16)

Chart 6

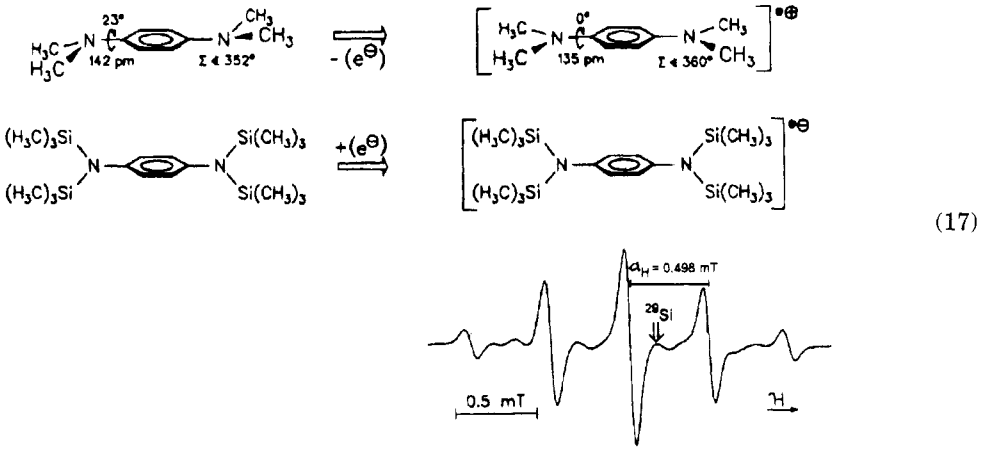

(17)

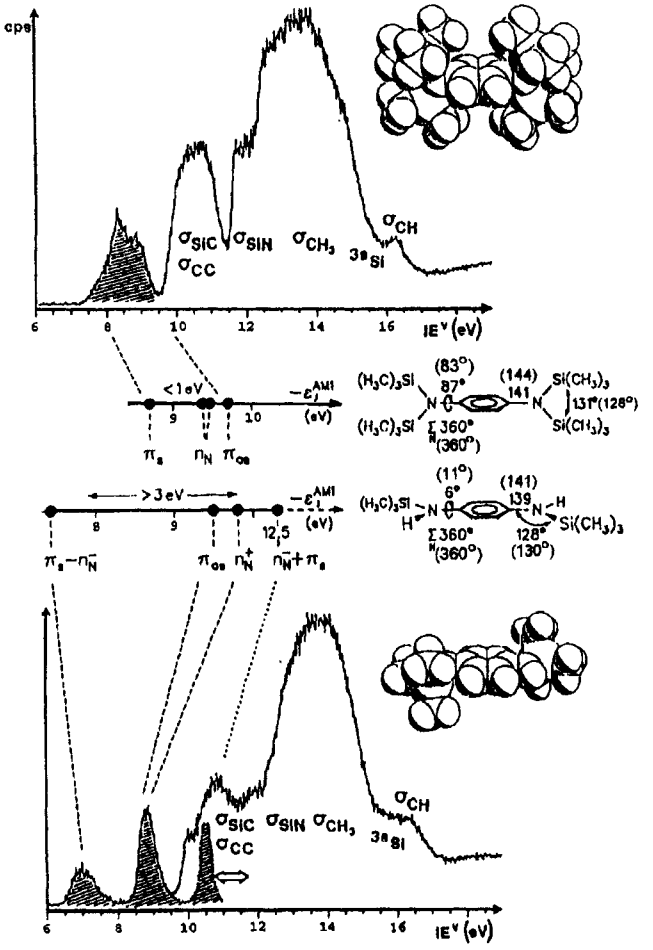

Figure 16. He I photoelectron spectra (6–18 eV) of *N,N'*-bis(trimethylsilyl)- and *N,N,N',N'*-tetrakis(trimethylsilyl)-*p*-phenylenediamines with Koopmans' assignment, $IE_n = -\epsilon_j^{AM1}$, based on the eigenvalues of geometry-optimized AM1 calculations, the structural data of which are given. Also shown are space-filling representations of the single crystal structures carried out for the neutral molecules (values in brackets; cf. the text).

the flattened conformation of *N,N'*-bis(trimethylsilyl)-*p*-phenylene diamine which shows a gauche arrangement and an astounding widening of the angle CNSi to 130° (Figure 16).

For gas phase structure determinations by quantum chemical evaluation of the sequences of the radical cation state recorded (section II.3), the two silyl-substituted p-phenylene diamines with their tremendously differing structures provide a "par excellence" example:[57,58] The photoelectron spectra of both compounds (Figure 16) exhibit n_N/π ionization band splittings either smaller than 1 eV or larger than 3 eV and suggest that the gas phase structures as deduced from the geometry-optimized AM1 calculations for the assignment of their ionization patterns must resemble approximately those in their crystal.[57] The sterically congested tetrakis(trimethylsilyl)-*p*-phenylenediamine should also be twisted in solution. Because of both the zero n_N/π donation and the considerable σ-acceptor perturbation of the benzene ring due to the high effective nuclear charge of the adjacent N centers, electron insertion to the "Wurster's Blue" radical anion can be achieved, as had been correctly anticipated in planning the ESR experiment (Chart 6).

The PES investigations have included less overcrowded molecules such as 1,4-bis(trimethylsiloxy)-benzene, which however still exhibits intramolecular interactions between trimethylsilyl and ortho ring hydrogens (Figure 17).[59]

1,4-Bis(trimethylsiloxy)benzene has been crystallized both by vacuum sublimation and from n-heptane solution. Both methods yielded colorless plates of the same monoclinic modification,[60] in which the molecular conformation of C1 symmetry shows the two $(H_3C)_3SiO$ substituents to be conrotationally twisted around the OC_6H_4O axis by dihedral angles of ±60° (Figure 17A). According to photoelectron spectroscopic ionization pattern and its Koopmans' assignment, $IE_n^v = -\epsilon_j^{AM1}$, by AM1 eigenvalues, the molecular structure in the gas phase should also have C_1 symmetry (Figue 17C). Surprisingly, a comparison of geometry-optimized MNDO, AM1, or PM3 calculations for the monosubstituted model compounds $H_5C_6OSi(CH_3)_3$ does not support the 60° dihedral angle predicted from the Koopmans' correlation. The diverging results obviously demonstrate a borderline for semiempirical calculations of medium-sized molecules (section II.5): The enthalpy differences between the rather shallow minima (Figure 17B) are too small to be calculated correctly without including correlation. In conclusion, it is pointed out that the second-order perturbation of the benzene π system by two $(H_3C)_3SiO$ substituents

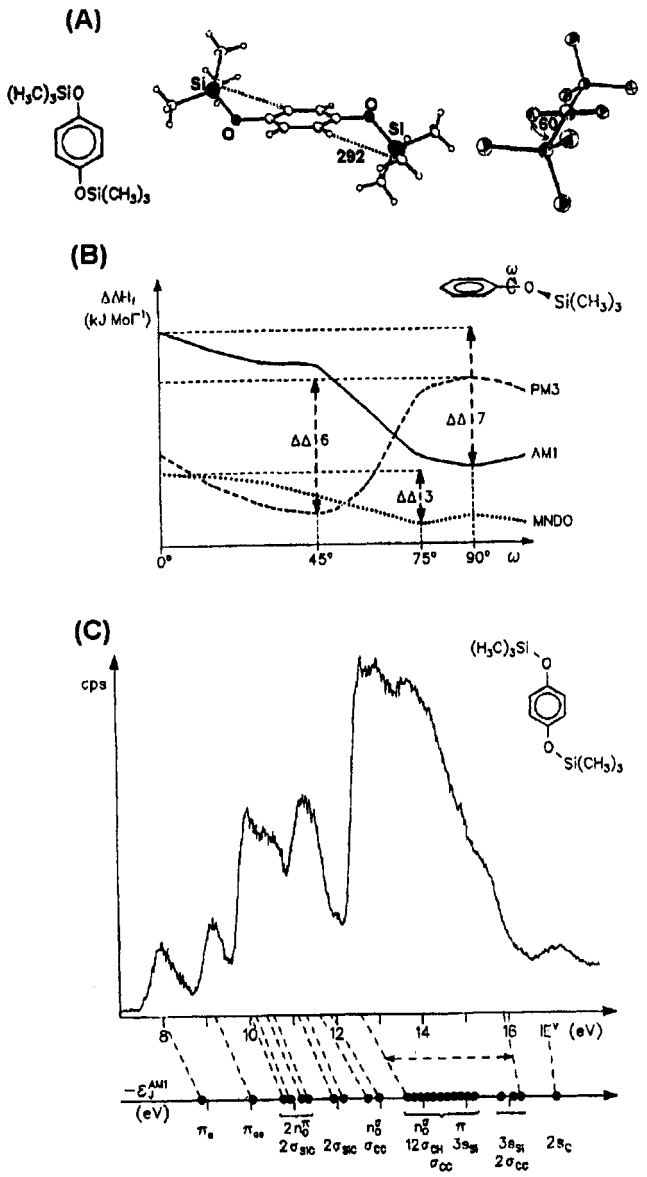

Figure 17. 1,4-Bis(trimethylsiloxy)benzene: (A) single crystal structure in side view and in axial view (50% thermal ellipsoids), (B) semiempirical one-dimensional enthalpy hypersurfaces for changes of the dihedral angle ω in the monosubstituted model compounds, and (C) photoelectron spectrum with Koopmans' assignment based on AM1 eigenvalues.

amounts to 9.24−7.96 = 1.28 eV at a 60° dihedral angle ($\cos^2 60° = 0.25$) and, therefore, approaches that of the $((H_3C)_3Si)_2N$ substituents (Figure 16).

Discussion of both the structural distortions due to supersilyl substituents and their electronic effects as exemplified by two rather recent investigations (Figures 16 and 17) should stimulate further intensified effort. Comparison of the first vertical ionization energies determined by photoelectron spectroscopy for a series of chemically related compounds such as methyl sulfides[51] (Figure 14 and (18)), methyl ethers[50] (Figure 15 and (19)), 1,4-benzene derivatives[50,61] (20), trans-1,2-disubstituted ethylenes[62] (21), disubstituted acetylenes[50,62,63] (22), and last, but not least, saturated disilane derivatives[50,58,64] (23) all prove without any exception that the bulky groups $C(Si(CH_3)_3)_3$ and $Si(Si(CH_3)_3)_3$ always cause the strongest lowering effect:

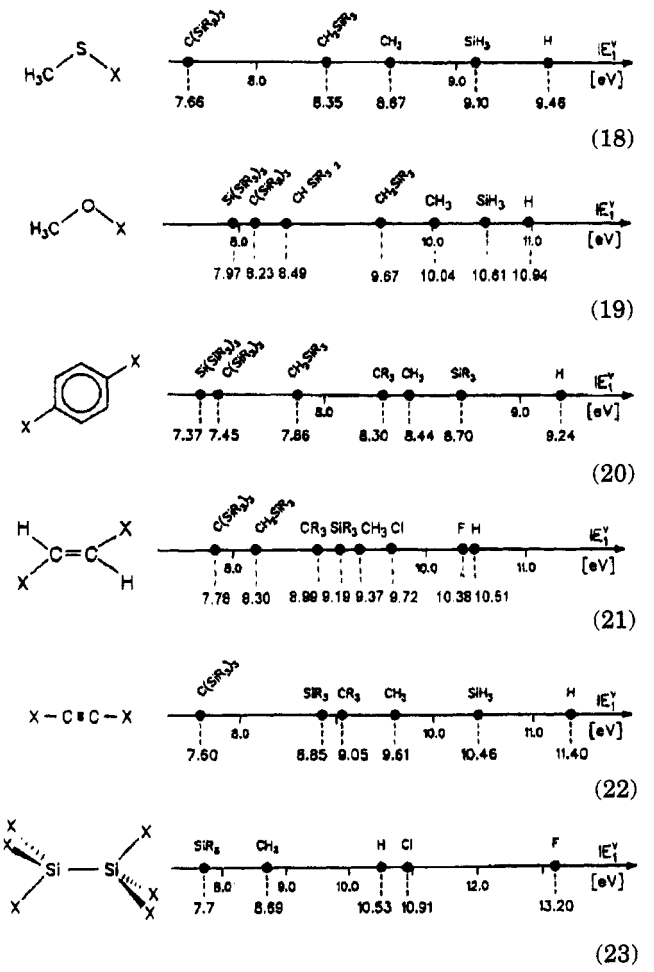

In the ground states of the radical cations generated, the delocalization of the positive charge is energetically favorable. In general, β-silyl half-shell substituents such as $C(SiR_3)_3$ and $Si(SiR_3)_3$ are excellent electron donors for molecules containing adjacent electron pair centers (18 and 19), for π systems (20−22), and even for σ skeletons such as the ones in polysilanes ((23) and Figures 5 and 6). The electron-donating effect can be traced back predominantly to the low effective nuclear charge of the Si centers,[2] which lowers the first vertical ionization energy of the parent compound by 1.8 eV for H_3CSH (18), 3.0 eV for H_3COH (19), 1.9 eV for benzene 1,4-disubstitution (20), 2.7 eV in (*E*)-1,2-ethylenes (21), 3.8 eV for HC≡CH (22), and 2.8 eV for disilanes (23). The latter exhibit further increases of 0.4 and 2.7 eV on Cl and F substitution, supporting the assumption of dominant effective nuclear charges.[64]

For the special case of hexakis(trimethylsilyl)-disilane, the topological σ_{SiSi} bond model with its parameter set α_{SiSi} = 8.7 eV and $\beta_{SiSi/SiSi}$ = 0.5 eV (section II.1, Figure 6) can be applied after introducing the additional Coulomb value $\alpha_{(SiSi)Si_6}$ = 9.05 eV for the central SiSi disilane bond: As shown in Chart 7, the band pattern in the low-energy PES ionization region can be deconvoluted to yield seven bands, the approximate maxima of which (Chart 7, IE_n^v (eV)) correlate satisfactorily with the topological eigenvalues $-x_J$ (eV). Within this context, it is pointed out that $Si(Si(CH_3)_3)_4$ has been remeasured[1,11] using various photon energies[65] and the previous assignment[11] confirmed by $X\alpha$ calculations.[65]

Chart 7

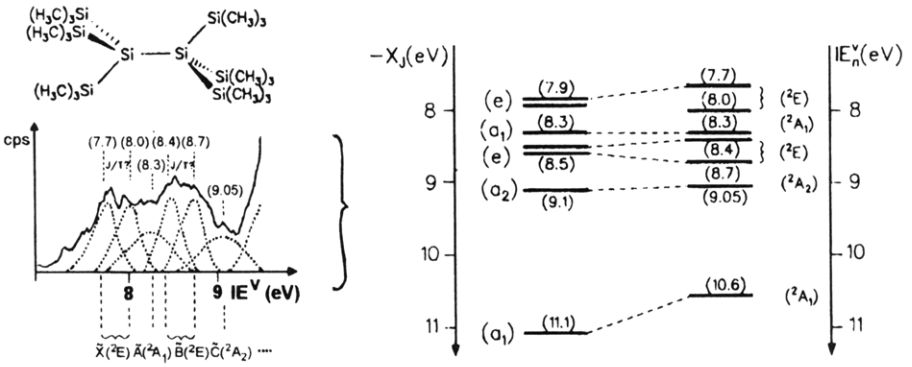

(24)

4. Silicocene and Metal Organic Silicon Derivatives

This section is opened with a discussion of the silicocene radical cation states[66] for two reasons. In the preceding report 1989,[1] only a preliminary personal communication could be included and, more importantly, the bis(η^5-pentamethylcyclopentadienyl)silicon sandwich exhibits a Si coordination number of 10, the highest observed so far.[2] The compound is synthesized by reacting bis(pentamethylcyclopentadienyl)silicon dichloride $(R_5C_5)_2SiCl_2$ with sodium naphthalide. The crystal structure proves two conformers, one with rings coparallel (D_{5d}) and the other one bent (C_{2v}) with an interplanar angle of 25°. Electron diffraction in the gas phase yields an average (large amplitude motion) value of 23°.[66] The novel compound could be evaporated and its PE spectrum recorded (Figure 18).

By SCF calculations on the probably insufficient STO-3G level, the twisted conformer Ia of C_s symmetry is predicted to be a global minimum, with **Ib** and **Ic** differing only by 5−6 kJ mol^{-1}. On the other hand, both the different steep−broad−steep band contours (Figure 18) and the $M^{\bullet+}$ state comparison with the Ge and Sn derivatives leave no doubt that the sequence of the three lowest vertical ionizations of silicocene (in orbital notation for D_{5d} symmetry) is $\pi(3e_{1g}) < 3s_{Si} + \pi < \pi(3e_{1u})$. The doublet radical cation ground state $\tilde{X}(^2E_{1g})$, therefore, by symmetry arguments has its positive charge exclusively delocalized within the π system of the pentamethylcyclopentadienyl ligand.

A closely related example with silicon of coordination number 6 is that of 1,2-dimethyl-1,2-disila-*closo*-dodecaborane(12),[67] the PE spectrum of which can also be recorded at 10^{-5} mbar pressure using a heated inlet system (Figure 19).

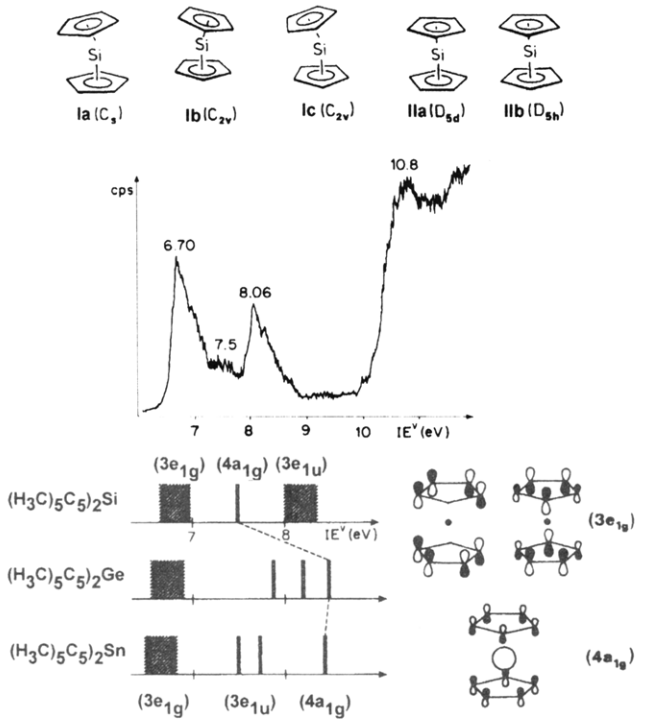

Figure 18. He I PE spectrum (6−10 eV) of bis(η^5-pentamethylcyclopentadienyl)silicon as the most likely conformer **Ia** (cf. the text) and its assignment by both Koopmans' correlations, $IE_n{}^v = \epsilon_j{}^{MNDO}$, as well as by radical cation state comparison with its Ge and Sn analogues (cf. the text).

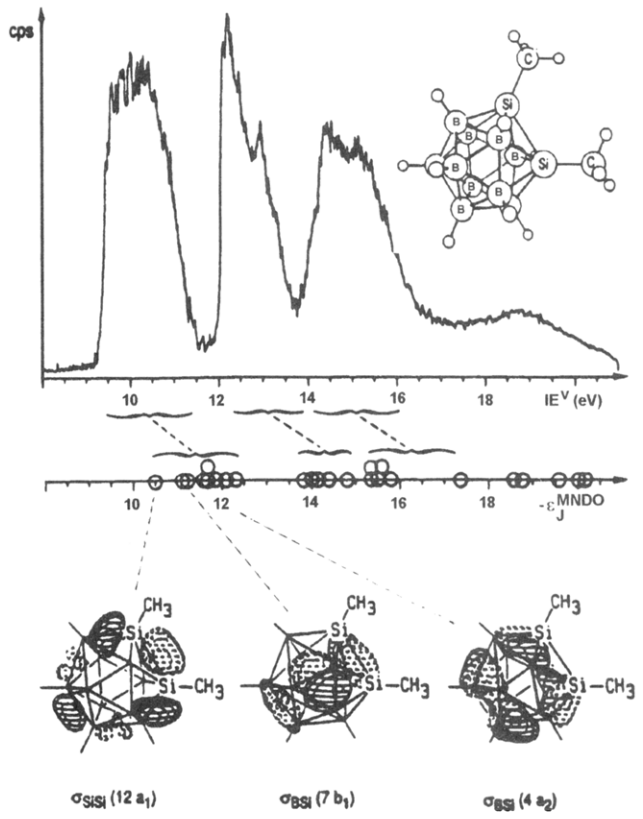

Figure 19. He I PE spectrum of 1,2-dimethyl-1,2-disila-*closo*-dodecaborane(12) ($(H_3CSi)_2B_{10}H_{10}$) with Koopmans' assignment by MNDO eigenvalues and cluster orbital diagrams for the three radical cation states of lowest energy.

Following the literature assignment[67] for the parent *closo*-dodecaborane(12) $(HC)_2B_{10}H_{10}$ framework, in addition to 13 cluster and 10 BH ionizations, a further 14 are expected for the two H_3CSi subunits. On the basis of the relative He I photoelectron spectroscopic band intensities (Figure 19) about 25 ionizations with predominant atomic contributions 2s, p_B, $1s_H$, $3p_{Si}$, and $2p_C$ are observed within the He I measurement region. The recommended[67] geometry-optimized MNDO calculations suggest that the ionizations of lowest energy can be grouped into nine cluster-type transitions within the band hill between 9.5 and 10.5 eV, five of BH and SiC character within the bands overlapping between 12 and 13.5 eV, and another five of predominant BH and CH contributions within the double band region between 14 and 16 eV (Figure 19). Although the overall PES band pattern is satisfactorily reproduced by the Koopmans' correlation, $IE_n^v = \epsilon_j^{MNDO}$, considerable Koopmans' defects, $\epsilon_j^{MNDO} - IE_n^v \approx 1.5$ eV, are calculated, indicating that the proposed sequence of the radical cation states assigned has to be viewed with some caution.

A comparison with the respective ionizations of the 1,2-carborane[67] demonstrates that upon replacement of the cluster CH subunits by $SiCH_3$ all three ionization regions are shifted to lower energies by at least 1.5 eV.[67] This observation can be traced again to the considerable decrease in effective nuclear charge from carbon to silicon centers.[2] Accordingly, silicon cluster subunits $SiCH_3$ are expected to act as electron donors even to the surrounding B(H) centers. This assumption is substantiated by the calculated MNDO charge distributions for both 1,2-carborane and 1,2-bis(silamethyl)-*closo*-dodecaborane(12), which suggest that the $(H_3C)SiSi(CH_3)$ subunit considerably increases the electron density within the $(BH)_{10}$ cluster framework and thus provides a plausible explanation for the remarkable 1.5 eV shift of the three separated bands to lower energy[67] (Figure 19).

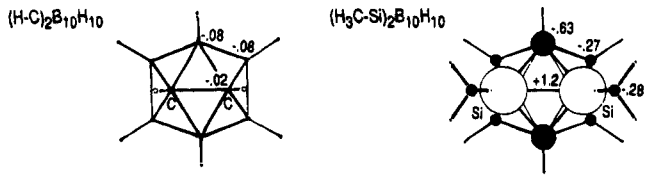

(25)

Summarizing, 1,2-dimethyl-1,2-disila-*closo*-dodecaborane(12), which exhibits in its PE spectrum the lowest ionization onset, 9.5 eV, observed so far for analogous compounds,[67] may be viewed as being presently the most electron-rich cluster, $XYB_{10}H_{10}$, with two adjacent main group element centers, XY.

Continuing with a reference to the PE spectrum of $Ge(Si(CH_3)_3)_4$, which has been recorded together with that of the already quoted analogous molecule $Si(Si(CH_3)_3)_4$,[65] we note that only few silicon containing metalorganic radical cation states have been investigated in the gas phase. The series of publications[68-70] discussed here first concerns information from photoelectron spectroscopic comparison on metal-catalyzed hydrosilylation:

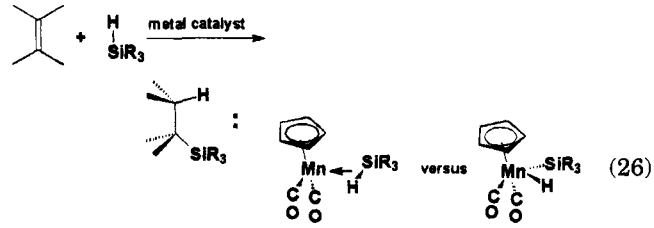

(26)

The PE spectra have been assigned on the basis of both reliable Fenske–Hall calculations as well as the partly impressive He I /He II intensity differences:[70] The Fe 3d photoionization cross sections, for instance, are predicted to rise by a factor of 1.6, while those of C 2p, Cl 3p, and Si 3p ionizations decrease on going from He I to He II excitation (Figure 20). In the corresponding manganese complexes (26) two possibilities for bonding exist, which are partly supported by neutron diffraction structures:[70] either a Mn (d^6) complex with $\sigma_{SiH} \rightarrow$ Mn donation or a Mn (d^4) oxidative addition product with both σ_{MnH} and σ_{MnSi} bonds. According to the PE spectra, the first is found with $HSiCl_3$ and the other with $HSiR_3$.[68,69] The SiH bond activation, unfortunately, is discussed exclusively within the fictional orbital approach[2,3] including even unoccupied σ_{SiH}^* and $3d_{Si}$ orbitals, which are useless for interpreting the PE spectra and radical cation states.

Within the review period 1988 to 1994, a Chemical Abstracts Service (CAS) on line search yielded only four further PE spectroscopic investigations of silicon-containing organometallic compounds (R = CH_3):[71-73]

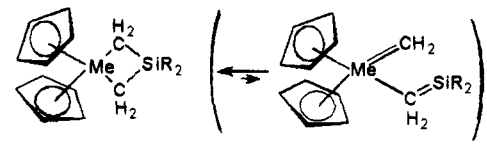

Me[71] : Ti, Zr, Mo, Th

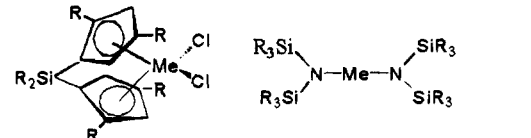

Me[72] : Zr, Hf, Fe Me[73] : Mn, Fe

(27)

He I /He II PE spectra suggest that the bis(η^5-cyclopentadienyl)-1-sila-3-metallacyclobutanes can be evaporated under reduced pressure without ring opening.[71] The X-ray PES investigation of Zr $3d_{5/2}$, H_f $4f_{7/2}$, and Fe $2p_{3/2}$ ionizations shows that the binding energies decrease by about 0.1 eV per R_3Si group. The PE spectra of bis(bis(trimethylsilyl)-amido)manganese and iron are assigned by comparison with analogous compounds, showing metal 3d ionizations at 7.9 eV and those from the nitrogen lone pairs at 8.5 eV.[73]

Altogether, radical cation states containing silicon centers with coordination numbers as high as 10 in silicocene (Figure 18) or 6 in disilacarbene (Figure 19) can be discussed within Koopmans' correlations with SCF eigenvalues. The same applies to metalorganic derivatives, for which metal d ionizations are advantageously assigned based on He I /He II intensity differences (Figure 19).

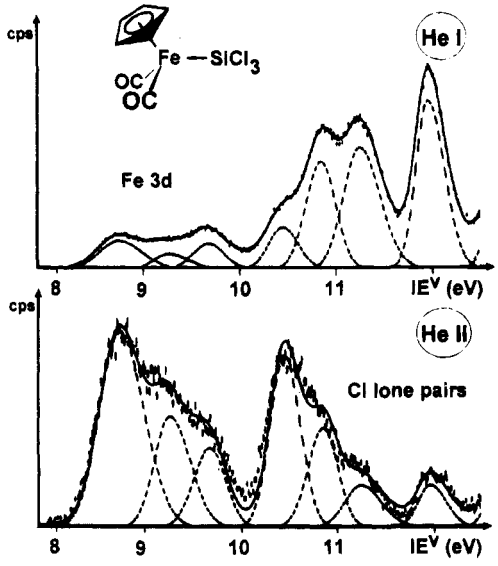

Figure 20. He I/He II trends in the PE spectra (8–12.5 eV) of $(\eta^5\text{-}C_5H_5)Fe(CO)_2SiCl_3$ due to the different cross sections[70] of Fe 3d and Cl lone pair ionizations.

5. Compilation of Vertical Ionization Energies since 1989

Referring to the more detailed discussions of the preceding topics—silylenes with Si of coordination number 2 (section III.1), siloxanes and silthianes with n_O and n_S lone pairs (section III.2), and compounds with bulky organosilicon substituents, e.g. coordination numbers as high as 10 or 6 (section III.4)—the remaining gas phase investigations resulting from the CAS on line search of data from 1989 to 1994 are listed with characteristic ionizations according to the type of compound[1] (Table 1) and commented on below.

The molecules and their first vertical ionization energies listed (Table 1) supplement those already presented as examples. The parent silylene has been generated by $SiH_4 + 2F^\bullet \rightarrow SiH_2 + 2\ HF$ and investigated by photoionization mass spectroscopy (PES), which yields the adiabatic onset value quoted.[74] Numerous molecules with 2-fold coordinated silicon, including some that are stable at room temperature, are known (section III.1) The silyl derivatives such as $C(SiH_3)_4$ have been thermally decomposed to detect new routes to amorphous, hydrogen-containing silicon, a promising new material.[75] The precise redetermination of the methylsilane ionization using synchrotron radiation[65] should be augmented by remarks pointing to both the simultaneous vibrational $2p_{Si}$ core level measurements[85] and also to the correlated calculations on Jahn/Teller distortions, e.g. for $SiH_4^{\bullet+}$ and $Si(CH_3)_4^{\bullet+}$.[86] Other polysilanes were presented under various aspects [cf. Figures 4–6 or (23) and Chart 7]. Both chlorofluorosilanes have been prepared by reacting Na_2SiF_6 with $(AlCl_3)_2$.[76] The differences in ionization energies of cyclic perchlorosilanes $[(SiCl_2)_{4-6}]$ may be rationalized by their geometry-optimized, calculated structures of D_{4h}, C_1, or D_{3d} symmetry.[77] The pyrolyses of the trimethylsilyl esters yielded mixtures,[78] containing R_3SiF and R_3SiOH,[78] which is of interest for comparison with the oxygen derivatives discussed in detail [section II.2, Figures 14, 15, and 17, Chart 4, and (18), (19)].

Table 1. Survey of Additional Photoelectron Spectra Recorded for Organosilicon Molecules from 1989 to 1994 Arranged According to Compounds Type[1] [cf. (18)–(23)]

compound (R=CH_3)	references	IE_1^v (eV)
(1) σ-Type Molecules		
SiH_2	74	(8.2), onset $\tilde{X}(^1A_1)$
$C(SiH_3)_2HR$	75	10.30, $\tilde{X}(^2A'')$
$C(SiH_3)_3H$	75	10.58, $\tilde{X}(^2E)$
$C(SiH_3)_4$	75	10.75, $\tilde{X}(^2T_2)$
SiR_4	65	10.35, $\tilde{X}(^2T_2)$
$Si2R_6$	65	8.45, $\tilde{X}(^2A_1)$
$Si(SiR_3)_4$	65	8.26, $\tilde{X}(^2T_2)$
$Ge(SiR_3)_4$	65	8.13, $\tilde{X}(^2A_2)$
$(SiR_2)_6$	65	7.89, $\tilde{X}(^2A_{1u})$
(2) Halogen Derivatives		
SiF_2Cl_2	76	12.66, $\tilde{X}(^2B_1)$
$SiFCl_3$	76	12.21, $\tilde{X}(^2A_2)$
$(SiCl_2)_4$	77	8.85, $\tilde{X}(^2B_{2g})$
$(SiCl_2)_5$	77	9.50, $\tilde{X}(^2A)$
$(SiCl_2)_6$	77	9.00, $\tilde{X}(^2A_{1u})$
R_3SiF	78	11.00, $\tilde{X}(^2E)$
(3) Group VI Derivatives		
R_3SiOH	78	10.00, $\tilde{X}(^2A)$
$R_3SiOSO_2CF_3$	78	(10.0)
$R_3SiOCOCF_3$	78	(10.9)
$R_3SiOCOCH_3$	78	(10.2)
$XSi(OCH_2CH_2)_3N$	79	
X = CH_3		8.5, σ_{SiN}
X = CH_2Cl		9.2, σ_{SiN}
X = $HC{=}CH_2$		8.5, σ_{SiN}
X = Cl		9.6, σ_{SiN}
X = F		9.7, σ_{SiN}
(4) Group V Derivatives		
$C_6H_5Si(NCO)_3$	80	9.73, $\tilde{X}(^2E_{1g})$
$(PSiCR_3)_4$	81	7.6, $\tilde{X}(^2E) + \tilde{A}(^2B_2)$
$(C_6H_5)_2XSiR_3$	82	
X = N		7.44, n_N
X = P		7.74, n_P
X = As		7.72, n_{As}
X = Sb		7.66, n_{Sb}
$C_6H_5HNSiR_3$	83	7.70, n_N
$(C_6H_5)_2NSi(C_6H_5)_3$		7.32, n_N
$(C_6H_5)_2NSi(C_6F_5)_3$		8.07, n_N
(5) Carbon π Systems		
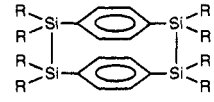	84	7.8, $\tilde{X}(^2B_{3u})$
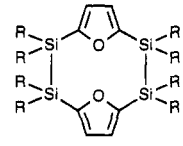		7.4, $\tilde{X}(^2A_u)$
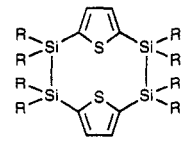		7.4, $\tilde{X}(^2A_u)$

The publication quoted for the silatranes,[79] which contain silicon of coordination number 5, reports on a total of 17 derivatives with partly substituted alkyl chains or groups. The lower ionization energies for isothiocyanates relative to cyanates have been reported before[1] and amount to $\Delta IE_1^v = 1.56$ eV for the parent molecules H_3SiNCX and to 1 eV for the larger methylated species R_3SiNCX.[80] Tetraphosphatetrasilacubane, $[PSiC(CH_3)_3]_4$, has been synthesized from $(H_3C)_3CSiCl_3$ and $Li^+[Al(PH_2)_4]^-$ and its ioniza-

tion is 0.25 eV higher than that of its carbon analogue, $[PCC(CH_3)_3]_4$.[81] In the group IV diphenyl(trimethylsilyl) derivatives $[(H_5C_6)_2XSiR_3]$, the second, benzene-π_{as}-assigned ionization energy remains constant, as expected.[82] For *N*-phenyl derivatives, the discussion of the conformers of *p*-phenylenediamines $(R_3Si)_nH_{2-n}NC_6H_5NH_{2-n}(SiR_3)_n$ (Figure 16) is noteworthy.[57] The discussion[82] includes the intensity ratios of He I /He II bands (Figure 20). The paracyclophane derivatives, quoted last but not least,[84] convey another example of π-perturbation, as has been discussed for first- and second-order perturbations (Figure 10) through out this third section [cf. Figure 7, Charts 1 and 2, and (8) and (20)–(22)], which provides an update of the previous review[1] up to the end of 1994.

IV. Recent Investigations of Organosilicon Cations in Solvents

Frequently, the gas phase measurement of the first vertical ionization energy preceded the generation of the radical cation in solution (Figure 8).[1,2,16] Especially when the selective, oxygen-free, and powerful redox reagents $AlCl_3/H_2CCl_2$ or $SbCl_5/H_2CCl_2$ have been applied,[17] the correlation with $IE_1^v < 8$ eV for a successful one-electron transfer never failed to yield persistent paramagnetic species (Figures 7, 8, and 11). The above redox systems have the additional advantage of allowing ENDOR[8] and especially ^{29}Si-ENDOR spectroscopy[12] (Figure 8) in the resulting methylenedichloride solutions. In addition, matrix isolation techniques[87] have proven valuable for investigations of rather reactive intermediates.

1. Matrix Isolation

The application of matrix techniques to investigation of organosilicon compounds, including the already mentioned matrix photolysis of phenyltriazidosilane ($H_5C_6Si(N_3)_3$) to phenylsilaisonitrile (H_5C_6-N≡Si)[13] (cf. Figure 9) were included in the preceding review[1] and, therefore, will be introduced here by another "classical" σ and π example of each[88–92] (Figures 21 and 22).

Starting from the photoelectron spectrum of tetramethylsilane,[1] which has been assigned assuming a Jahn/Teller distortion from T_d symmetry,[86] the radical cation $Si(CH_3)_4^{\bullet+}$ has been generated in the matrix. The ESR signal pattern consists of a septet of septets due to two pairs of equivalent, freely rotating methyl groups, which thus excludes distortions $T_d \rightarrow D_{4h}$ or $T_d \rightarrow D_{2d}$. A satisfactory rationale[88] for the most likely structural change on one-electron expulsion, $T_d \rightarrow C_{2v}$, is provided by the predicted orbital splitting, $1t_1 \rightarrow 2a_1$ (↑) > $1b_2$ (↑↓) > $1b_1$ (↑↓).

For silyl-substituted ethylene radical cations, quantum chemical calculations predict that the two molecular halves are twisted around the central C=C bond[90,91] by about 30°, lowering the total energy by about 5 kJ mol^{-1} (cf. also ref 4). The recorded ESR multiplets (Figure 21) with *g* values between 2.0031 and 2.0038 fulfill these expectations. For the CH_2 hydrogens, a triplet with $a_H = 4.42$ mT results, while for single hydrogens (CHR), doublets with $a_H = 4.53$ and 6.45 mT are observed. According to the open

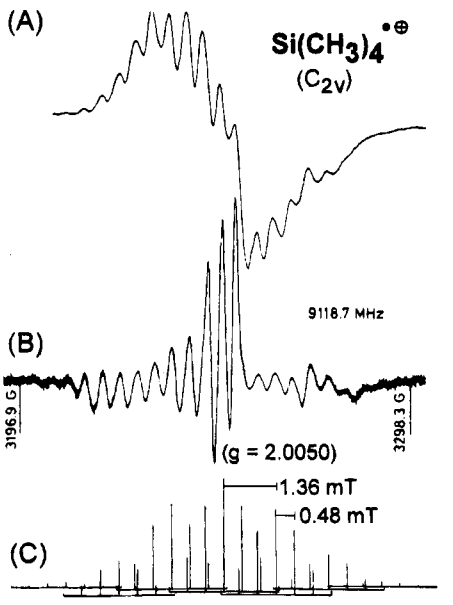

Figure 21. Tetramethylsilane radical cation in 8% mol solid solution in trichlorofluoromethane at 90 K, generated by γ-irradiation (dose, 1 Mrad): (A) first- and (B) second-derivative ESR spectra as well as (C) stick diagram reconstruction consisting of a septet of septets showing the line component assignment.

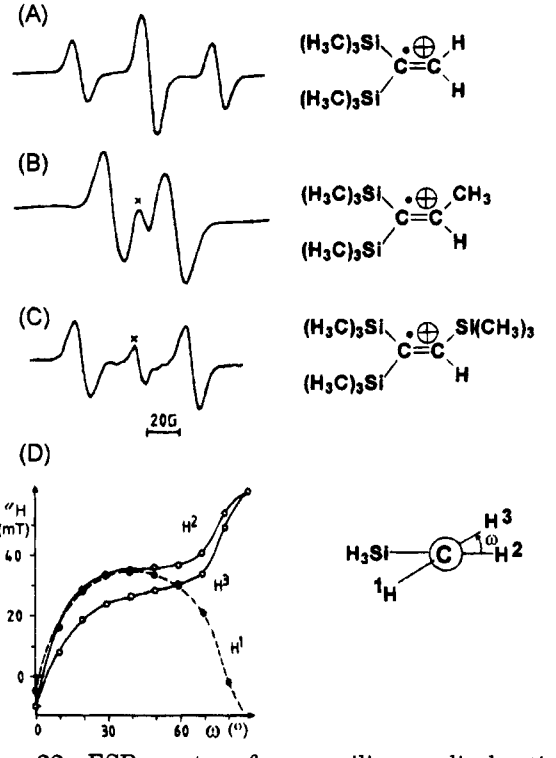

Figure 22. ESR spectra of organosilicon radical cations generated in trichlorofluoromethane matrices at 77 K by ^{60}Co γ-irradiation: (A) 1,1-bis(trimethylsilyl)ethylene, (B) 1,1-bis(trimethylsilyl)-2-methylethylene, and (C) 1,1,2-tris-(trimethylsilyl)ethylene (X, signals from unidentified species; cf. the text). (D) INDO open shell hypersurface for the dependence of the coupling constants a_H on the dihedral angle (ω) in vinylsilane.

shell INDO hypersurfce calculations as a function of the dihedral angle ω (Figure 22D; cf. Figure 11), the rather large ethylene hydrogen couplings recorded indicate the twisting. Analogous investigations have been performed for other prototype radical cations such as β-silyl-substituted ethylenes H_2C=$CHCH_2$-

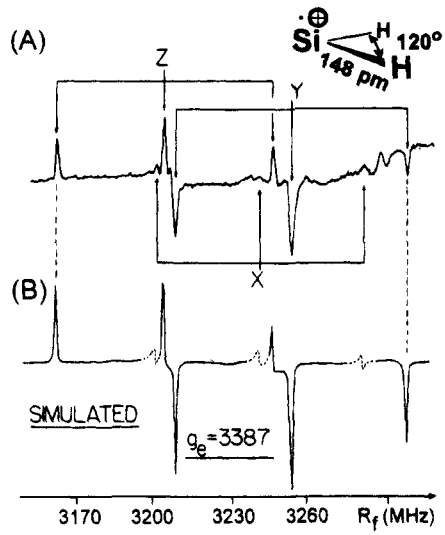

Figure 23. Silylene radical cation, $SiH_2^{\bullet+}$, generated by SiH_4 photolysis in a 4 K neon matrix: (A) low field part of the ^{29}Si (I = 1/2) ESR doublet hyperfine coupling in Θ = 90° position and (B) its simulation (for details, cf. ref 93).

SiR_3,[90] of benzene derivatives $H_5C_6SiR_3$ and H_5C_6-SiR_2SiR_3[92] or of siloxanes and silthiane derivatives.[92]

The literature search found no organosilylene radical cations ($R_2Si^{\bullet+}$), but the parent ($H_2Si^{\bullet+}$) has been generated in a neon matrix at 4 K by photoionization of SiH_4 and the solid state ESR recorded for its $\tilde{X}(^2A_1)$ ground state (Figure 23).

The **A** tensor assignment was facilitated by isolation of preferentially oriented $SiH_2^{\bullet+}$ in a neon lattice, and all the X, Y, Z components were resolved as demonstrated by the spectrum simulation (Figure 23B). In addition, correlated wave function calculations on the MP4 level confirm the exclusive generation of $SiH_2^{\bullet+}$ and exclude $SiH_4^{\bullet+}$ or $SiH^{\bullet+}\cdots H_2$. An angle $\angle$HSiH = 120° and bond lengths d_{SiH} = 148 pm are predicted.

A variety of alkylsilane radical cations have been investigated.[94-96] Radicals from $H_3Si(CH_2)_{n=1,2,3}CH_3$, $(H_3C)H_2Si(CH_2)_{n=1,2}CH_3$, and $H_2Si(CH_2CH_3)_2$[94] have been generated in a 77 K matrix of F_3CCCl_3 by ^{60}Co γ-irradiation. Their ESR spectra can be approximated by INDO open shell calculations, e.g. for $H_3CH_2CH_2SiCH_3$ (OH couplings observed experimentally; calculated ones in brackets):

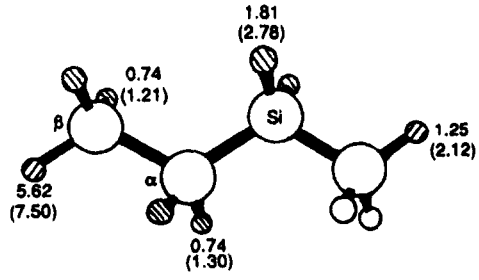

(28)

The reasonable correlation between experimental and calculated coupling constants (28, $a_H/(a_H)$) demonstrates that the largest effect is observed for the β-trans hydrogen, which encounters the largest (hyperconjugative)[94] transfer of spin predominantly located in the Si–C_α bond. Molecular dynamics are indicated by the temperature depencence of ESR signal patterns of 1-methylsilacyclohexene and silacyclobutane radical cations, generated in C_7F_{16} matrices at 77 K by γ-irradiation.[95,96] The experimental data can be rationalized by two-site jump models, in which either a distorted bond is dynamically moved to an equivalent position[95] or a ring-puckering motion activated[96] (coupling constants in brackets):

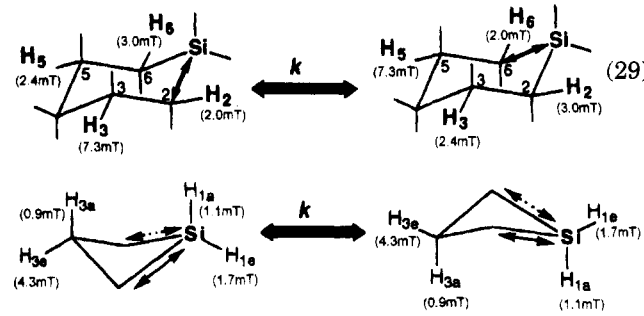

(30)

Another study in $FCCl_3$ matrices at 77 K compares analogous tin and silicon radical cations and their different stability. Whereas the (*p*-methoxybenzyl)-tributyltin radical cation on temperature increase splits off a benzyl radical:[97]

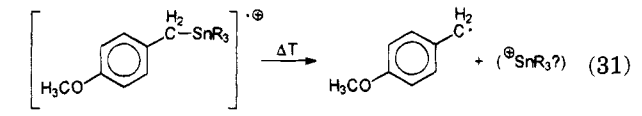

(31)

No such decomposition is observed for the analogous silicon derivative even upon heating the matrix up to its melting point.[97] For $H_5C_6SiCl_3^{\bullet+}$, the ESR multiplet suggests—as is expected by perturbation arguments (section II.4, Figure 10)—that the spin population can be rationalized by a single occupied π_{as} benzene orbital and, therefore, the Cl_3Si group acts as an acceptor substituent.[98]

Other hetero-organosilicon radical cations and especially nitrogen derivatives might be studied as well by the ^{14}N coupling (I = 1; natural abundance, 99.63%), which provides additional information. Their generation is accomplished straightforwardly by ^{60}Co γ-irridiation in $FCCl_3$ matrices[99] (isotropic N coupling constants A_{iso} in mT; R = CH_3):

	$(R_3Si)_nN^{\bullet\oplus}R_3$			$(R_3Si)_2N^{\bullet\oplus}=N(SiR_3)_2$	$R_3Si-\overset{\bullet\oplus}{N}-N=N$	
	n = 1	2	3	(ω ~ 240)	(-3.3)	
A_{iso}(mT)	16.0	15.0	14.3	10.3	10.7	4.0

(32)

The N coupling in the trimethylsilylamine radical cations is smaller than that observed for the corresponding alkyl derivatives (e.g. $(H_3C)_3N^{\bullet+}$: A_{iso} = 18.3[99]), The matrix-isolated tetrakis(trimethylsilyl)-hydrazine radical cation exhibits less twisted molecular halves than in solution (section II.2, Figure 11, $\omega \approx 45°$) and the trimethylsilyl azide radical cation has by far the highest spin population at the nitrogen center adjacent to silicon[99] (32).

In summary, ESR investigations of organosilicon radical cations in inert matrices, generated at rather low temperatures, can be considered to be a comple-

Chart 8

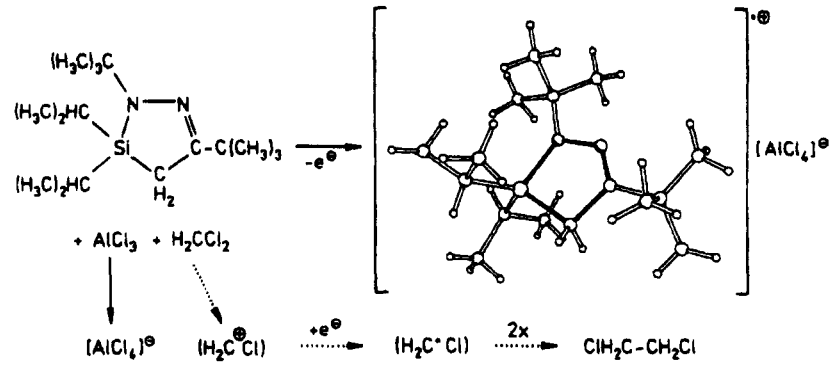

(33)

mentary method to vertical gas phase measurements, providing otherwise partly inaccessible and valuable information.

2. ESR/ENDOR Spectroscopic Investigations

Referring to the introductory "classical" examples (section II. 2), a large number of organosilicon radical cations[16] have been generated in $AlCl_3/H_2CCl_2$ solution by single electron oxidation from their neutral precursors, sometimes crystallized as radical cation tetrachloroaluminates, and their structures have been determined (Chart 8).[100]

Both the isolated and structurally characterized salt $M^{\bullet+}[AlCl_4^-]$ and the 1,2-dichloroethane identified by gas chromatography provide clues about the still unknown single electron transfer mechanism: Presumably, $AlCl_3$ will abstract Cl^- from H_2CCl_2, forming the counteranion $AlCl_4^-$. The resulting carbonium ion H_2CCl^+ could, upon selective single-electron transfer, yield the radical $H_2CCl^\bullet$, which should vanish in subsequent dimerization reactions to ClH_2C-CH_2Cl.[1,2,18] The same applies to the $SbCl_5/H_2CCl$ oxidation, which due to a slightly higher potential and 2:1 stoichiometry can be used to prepare numerous dication salts $[M^{2+}]$ $[SbCl_6^-]_2$ of main group element molecules M.[4] The oxidation potential of the $AlCl_3/H_2CCl_2$ single electron transfer system is approximately +1.7 V. By linear correlation based on nine sterically uncrowded compounds, $E^{Ox}(V) = -4.59 + 0.78IE_1^v$ (eV) with SE = 0.107, this corresponds to $IE_1^v = 8.0$ eV for gas phase ionization[1,2,18] (Figure 7). The first ionization potential of a promising precursor can either be found in the literature, predicted from heuristic correlations of suitable properties of chemically related molecules, estimated by fast semiempirical calculation, or even be recorded on an available photoelectron spectrometer within 1 h. Thus organosilicon radical cations[62] can be readily generated by the elegant addition of $AlCl_3$ to their H_2CCl_2 solutions (Figure 24). More time-demanding cyclovoltammetric measurements in aprotic (c_{H^+} < 1ppm) solution[101] provide criteria for reversible electron transfer processes such as a 59 mV distance between "forward and backward" peaks, which can be, but are not necessarily, indicative of whether the radical cation exhibits a lifetime long enough for ESR and especially for ENDOR characterization[8,16] (Figure 24). In addition, the same solution in H_2CCl_2, DME, DMF, or other solvents can be used to screen the reduction side for potential radical anion generation (Figures 24 and 25).

The assignment of ESR multiplet splitting, the "molecular state fingerprints" of radical cations (Figures 2, 8, 22–25), can be accomplished in many ways,[8] of which the following proved to be advantageous for those of organosilicon molecules: any ^1H, ^{13}C, and ^{29}Si ENDOR spectra allow a direct and precise read-off of the respective coupling constants from the line pair distances (Figure 8).[8,12] In case, the ESR signals cannot be saturated for ENDOR recordings, often the ESR line patterns can be simulated optimally by trial-and-error fit of varied

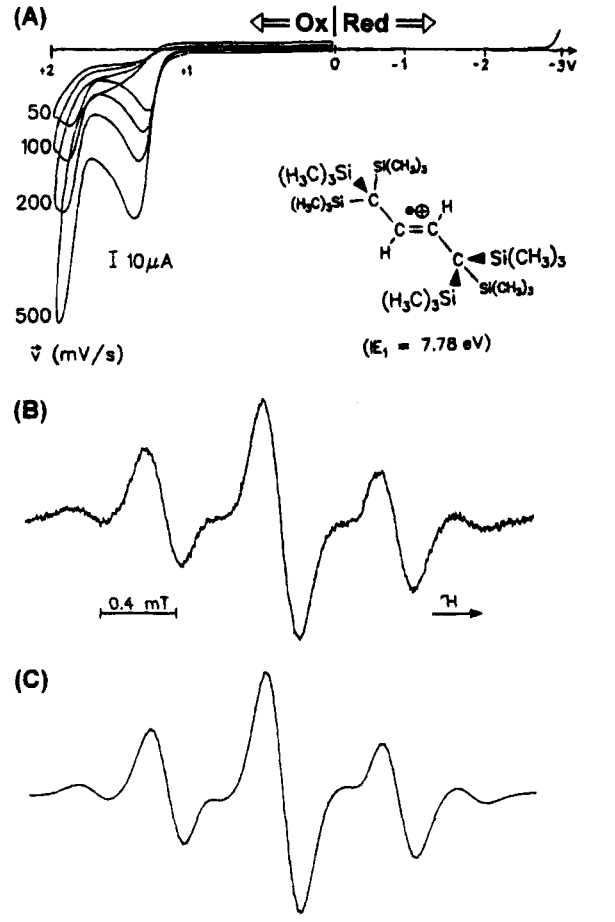

Figure 24. 1,1,1,4,4,4-Hexakis(trimethylsilyl)-2-butene (IE_1^v = 7.78 eV):[62] (A) cyclovoltammograms for oxidation (H_2CCl_2/0.1 M $R_4N^+ClO_4^-$, GCE vs SCE, recording velocity v = 50 to 500 mV/s) and reduction between 0 and −3 V (v = 100 mV/s), (B) ESR signal pattern of its radical cation generated with $SbCl_5$ in H_2CCl_2, and (C) optimized simulation with the trial-and-error coupling constants $a_H(CH)$ = 0.606 mT, $a_H(CH_3)$ = 0.022 mT, and a^{29}_{Si} = 0.767 for 2, 54, and 6 equivalent centers, respectively (see the text).

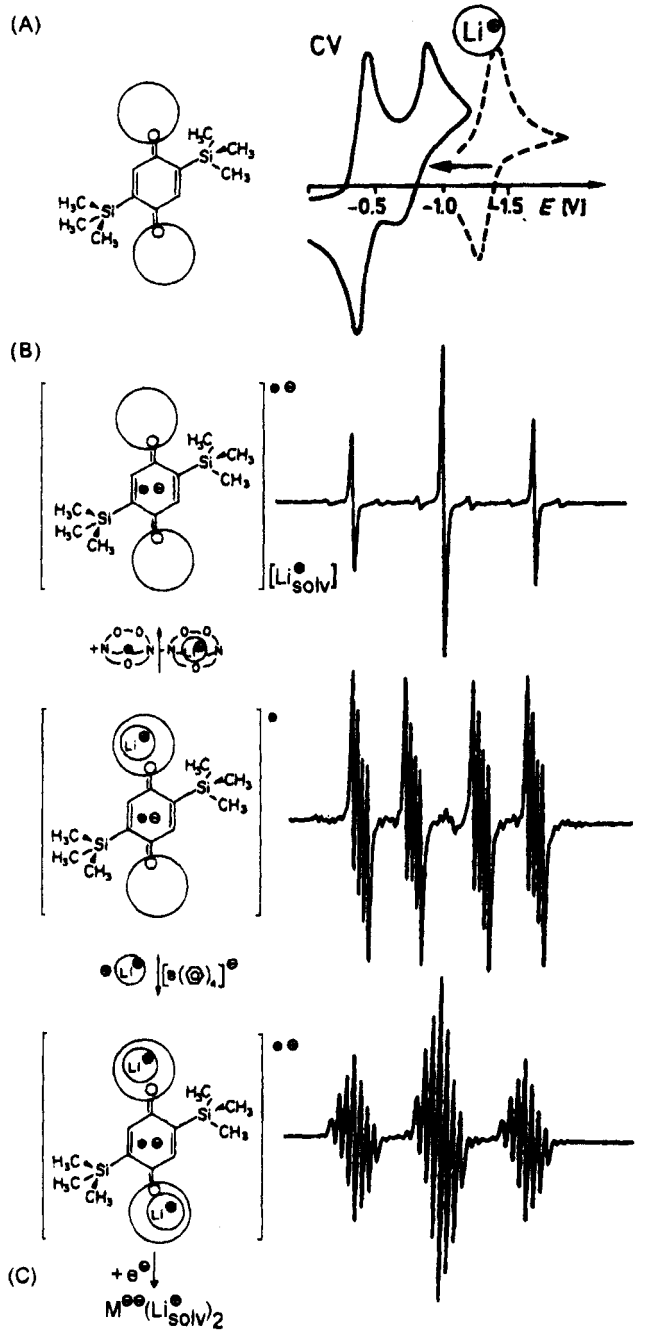

Figure 25. The two-electron reduction of 2,5-bis(trimethylsilyl)-*p*-benzoquinone in THF under aprotic (c_{H^+}) < 1 ppm) conditions: (A) cyclovoltammograms in THF with 0.1 M $R_4N^+ClO_4^-$ or $Li^+(B^-(C_6H_5)_4)$ as conducting salt (GCE vs SCE, v = 100 mV/s); (B) ESR spectra of "naked" 2,5-bis(trimethylsilyl)-*p*-benzoquinone radical anion, generated by lithium metal reduction in the presence of [2.1.1]-cryptand, of the radical $[M^{\bullet-}Li^+]^\bullet$ formed directly upon reduction with lithium metal and the triple ion radical cation $[Li^+M^{\bullet-}Li^+]^{\bullet+}$ prepared on increasing the Li^+ concentration in the THF solution by addition of the THF soluble salt $Li^+[B^-(C_6H_5)_4]$; and (C) addition of the second electron to the final reduction product, the dilithium salt of hydroquinone dianion.

coupling constants, some of which might be directly accessible from the high- or low-field satellites.[16] Sometimes molecular state comparison of related radical cations[16] or open-shell quantum-chemical calculations (Figure 11) provide hints.[16] For the ethylene radical cation,[62] substituted at both centers with bulky $C(Si(CH_3)_3)_3$ substituents, the ^1H- and ^{29}Si-coupling constants had to be determined by an optimized ESR spectrum simulation (Figure 24), because ENDOR saturation could not be achieved.

ESR and ENDOR spectra of organosilicon radical cations yield a wealth of partly otherwise inaccessible information[16] such as on the spin distributions, on structural changes during adiabatic relaxation, and on rigidity or flexibility within the ESR time scale of 10^{-7} s, orders of magnitude longer than the 10^{-15} s required for vertical ionization. Several spectacular effects have been discovered: for instance, the spin (and charge) distribution in the dodecamethylcyclohexasilane radical cation differs considerably from that in its radical anion:[102]

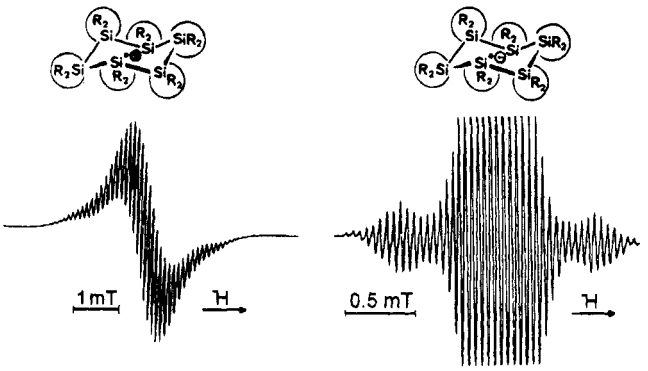

(34)

The high g value = 2.0093 for the radical cation reflects the spin population at the Si centers. The ESR multiplet (34) can be simulated satisfactorily by two different couplings of each 18 hydrogens indicating nonplanarity and some ^{29}Si coupling admixture.[102] In contrast, the radical anion exhibits a 37 line pattern due to either a planar $Si_6^{\bullet-}$ skeleton or rapid dynamic interconversion. The rather large observed ^{13}C coupling of 1.46 mT together with the value g = 2.0028 suggests a π-type radical anion with considerable spin (and charge) at the peripheral methyl groups.[102] Structural distortions are generally well-reproduced (Figure 11) or predicted by quantum-chemical calculations: For the period covered in this review, the energy hypersurface calculated for cyclotrisilane radical cation is emphasized,[103] on which both $(SiH_2)_3^{\bullet+}$ and $H_3SiHSi{=}SiH_2^{\bullet+}$ have been found in local minima.

Organosilicon radical cation dynamics, which can be determined in temperature-dependent ESR investigations,[16] cover the wide range from unhindered rotations in sterically unblocked derivatives via restricted cogwheel gearing in $(CH_3)_3SiCH_2)_3N^{\bullet+}$ (Chart 9A),[16] for which only two bulky $(H_3C)_3Si$ groups can be accommodated on the same side of the NC_3 plane and, therefore, both have to change places simultaneously to the completely blocked radical cation hexakis[(trimethylsilyl)methyl]benzene,[16] for which the tremendous overcrowding can be visualized by a space-filling structure representation (Chart 9B).[104]

Other structure determinations of neutral organosilicon compounds, from which radical cations have been generated and characterized by ESR spectroscopicy,[16] include $(R_3SiH_2C)_2C{=}C(CH_2SiR_3)_2$ [105] and $(R_3Si)_2C(HC{=}CH)_2C(SiR_3)_2$ [106] as well as $R_3SiN(RC{=}CR)_2NSiR_3$,[107] a dihydropyrazine derivative.

Chart 9

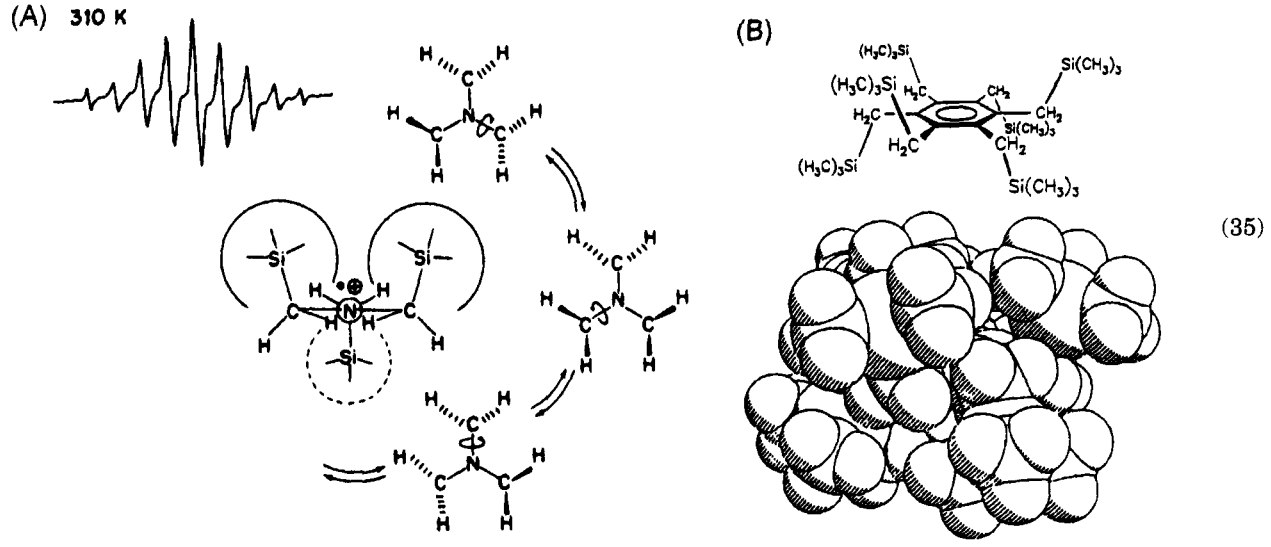

Continuing with the novel, ruby-colored hexakis-(trimethylsilyl)-2-butene radical cation[101] (Figure 24), the following information on electronic and dynamic radical cation properties can be extracted: Comparison of the CH hydrogen coupling constants proves that only dimethylamino groups are stronger electron donators.[1]

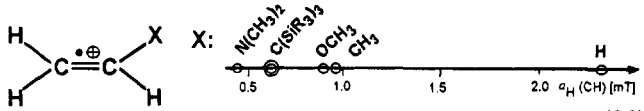

(36)

Applying the Heller/McConnell equation, $a_H = |Q_H|\varrho_c^{\pi}$ with the factor for π carbon radical cations $|Q_H| = 3.5$ mT, yields a π spin density $\varrho_c^{\pi} = 0.606/3.5 = 0.173$. For both C=C centers this amounts to 0.346 and suggests that about two-thirds of the total spin has been delocalized in the bulky substituents, $C(SiR_3)_3$! From a simplified approach, $a^{29}Si = B_2(Si)\langle\cos^2\Theta\rangle$, with the value $\langle\cos^2\omega\rangle = 0.5$ for free rotation and the ^{29}Si coupling of 0.767 mT measured, a parameter $B_2(Si) = 3.1$ mT results, which indicates that the bulky groups $C(SiR_3)_3$ can still rotate almost unhindered around the connecting C−C bonds.[101]

Within the review period, several *N*-trialkylsilyl derivatives have been oxidized by the powerful one-electron transfersystem $AlCl_3/H_2CCl_2$ (Figure 7 and Chart 8)[108-110] or by $Ag^+AsF_6^-$ [111] to their radical cations (R = CH_3):

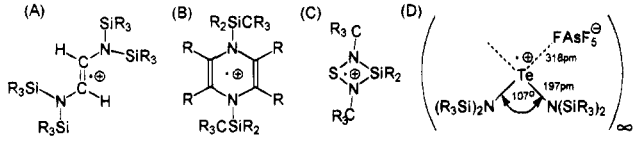

(37)

(*E*)-1,1,4,4-Tetrakis(trimethylsilyl)-1,4-diazabut-2-ene, which is prepared by complete reductive silylation of 2-(trimethylsilyl)-1,2,3-triazole,[108] upon $AlCl_3/H_2CCl_2$ oxidation yields, according to the ESR, a mixture containing the radical cation as the main component (37A). The permethylated dihydropyrazine derivative, the structure of which has been shown to be butterfly-shaped,[109] can be reversibly oxidized to its persistent radical cation as expected (37B). The octamethyl derivative of a 1-thia-3-sila-2,4-dimethyldiacetidine heterocycle is an electron-rich intermediate in the reductive cyclization of $R_3SiN{=}S{=}NSiR_3$ and can be oxidized to its radical cation (37C), exhibiting an ESR N quintet accompanied by ^{29}Si satellites. The blue radical cation of tetrakis(trimethylsilyl)telluriumdiamide, oxidized by $Ag^+AsF_6^-$ in H_2CCl_2 under silver metal powder deposition crystallizes in an orthorhombic cell with four formula units. The AsF_6^- anions connect the radical cations to an infinite string forming contacts with distances of 318 pm, which are about 11% shorter than the sum of the (Te + F) van der Waals radii.[111]

Altogether, within the review period, the pace of ESR/ENDOR investigations has not continued at previous levels and the hope is expressed that more information on the ground state properties of organosilicon radical cations, especially concerning spin delocalization phenomena, will be gathered in the future.

3. Reaction Intermediates

Microscopic reaction pathways for medium-sized molecules with N ≥ 6 centers, and, therefore, $3N - 6 \geq 12$ degrees of freedom are almost completely unknown.[112] In general this includes also quantum-chemical energy hypersurface calculations,[9] which would have to be carried out within the 12- or more dimensional hyperspace. In special cases, however, for some degrees of freedom higher activation barriers can be assumed and, therefore, the problem of the unknown reaction dynamics considerably simplified.[9,112] An illustrative example of experimental information gathered concerning a microscopic reaction pathway of medium-sized molecules is provided by the reduction of 2,5 bis(trimethylsilyl)-*p*-benzoquinone in THF solution to its hydroquinone derivative in the presence of soluble lithium salts such as $Li^+(B^-(C_6H_5)_4)$. Another type of a silicon containing radical cation (section IV.2) has been discovered by ESR spectroscopy[2,18,112] (Figure 25).

Chart 10

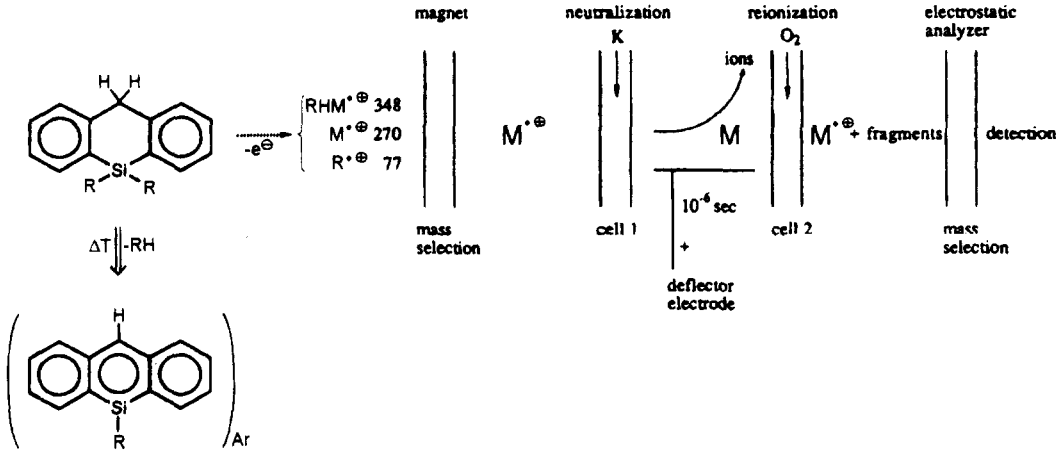

(38)

In detail, the cyclovoltammogram recorded for 2,5-bis(trimethylsilyl)-*p*-benzoquinone (Figure 25A) in aprotic THF or DMF solution containing tetra-*n*-butylammonium perchlorate as the conducting salt shows two completely reversible consecutive electron transfer steps. Exchanging the rather large, well-shielded R_4N^+ for the small, strongly solvated Li^+ counter cation lowers the second and now irreversible reduction potential by 0.6 V due to the formation of contact ion pairs, which can be observed by the changing ESR multiplet pattern of 2,5-bis(trimethylsilyl)-*p*-semiquinone radical anion in THF with increasing Li^+ concentration (Figure 4B): Reduction using lithium metal in the presence of [2.1.1]cryptand generates the "naked" radical anion $M^{\bullet-}$, for which the ESR 1:2:1 triplet proves two equivalent ring hydrogens. On reduction with lithium metal without a complexing agent, the ion pair radical $[M^{\bullet-}Li^+]^\bullet$ is formed, exhibiting a ^1H doublet of doublets with each line further split into a quartet for the one $^7Li^+$ (I = 3/2, natural abundance 92.58%) fixed into one of the two equivalent positions near the carbonyl subunits. Increasing the Li^+ concentration by addition of THF-soluble $Li^+(B^-(C_6H_5)_4)$ leads to the contact triple ion radical cation $[Li^+ M^{\bullet-}Li^+]^{\bullet+}$, as proven by the splitting of the ^1H triplet lines into septets due to the two $^7Li^+$ ions in equivalent positions near the negatively charged carbonyl oxygens of the semiquinone and formation of a most likely precursor for the second electron insertion to the final product, the dilithium salt of 2,5-bis(trimethylsilyl)hydroquinone (Figure 25C).

In general, application of the appropriate physical measurement techniques from the tremendous array now available from the armory of physics makes it possible to prove the existence of numerous reaction intermediates previously only suspected. For organosilicon radical cations, the literature search produced entries for the application of neutralization–reionization as well as collisional activation mass spectroscopy,[113-116] ion cyclotron resonance mass spectroscopy,[117] or chemical-induced dynamic nuclear polarization (CIDNP) NMR[118] techniques.

Starting with 9-silaanthracenes, the radical cations $M^{\bullet+}$ have been generated in the gas phase from 9,10-dihydrosilaanthracene precurcors by neutralization–reionization mass spectroscopy and their thermodynamical stability proved. The neutral compounds have been prepared by flash vacuum pyrolysis and isolated in a 15 K argon matrix (e.g. R = C_6H_5) (Chart 10).[113]

The self-explanatory Chart 10 shows the m/z selection of the radical cations $RHM^{\bullet+}$, $M^{\bullet+}$, and $R^{\bullet+}$ generated by electron ionization, their neutralization by K atoms, and their reionization by oxygen. On isolation in 15 K Ar matrices after preparative flash vacuum pyrolysis (Chart 10, ΔT), the neutral silaanthracene derivatives (R = H, C_6H_5) exhibit characteristic electronic absorptions between 27,600 and 19 500 cm^{-1}.[113]

In other neutralization–reionization and collisional activation experiments, the isolation of rather short-lived intermediates has been replaced by partly high level calculations of correlated wave functions. Chemical ionization with 70 eV electrons either of $H_5C_6SiH_3$ or of the mixture $C_6H_6/Si(CH_3)_4$ produces radical cations $\{H_6C_6Si\}^{\bullet+}$, for which open shell MP2/631G**//UHF/321G* calculations suggest as a sequence of decreasing stability from the π-complex: $\{Si^{\bullet+}(^2P) \cdots C_6H_6\} > H_5C_6SiH^{\bullet+} > (HC)_6Si^{\bullet+}$.[114] Starting from $Si(OCH_3)_4$, 70 eV electron impact ionization produced radical cations such as the distonic $^\bullet H_2COSi^+$, which can be neutralized at high collision energies to the biradical $^\bullet H_2COSi^\bullet$.[115] In addition, investigations of carbon-free species such as $HSiO^\bullet$ and $HSiO^+$, also generated on 70 eV electron impact from $Si(OCH_3)_4$,[116] or such as the radical cation $SiO_3^{\bullet+}$, generated by the reaction of $SiO_2^{\bullet+}$ with N_2O,[117] are pointed out.

The CIDNP technique has been used to obtain additional information on the photochemical reaction between *p*-benzoquinone derivatives and hexamethyldisilane in chloroform solution, which yields the mono- or bis(trimethylsilyl)hydroquinone derivatives and R_3SiCl (Chart 11).[118]

In the absorptive CIDNP phase during irradiation with a 1 kW high-pressure mercury lamp, three new NMR signals are observed, which suggest the following "in solvent cage" reaction pathway: The quinone excitation yields the triplet state, which is reduced by R_3SiSiR_3 (IE_1^v = 8.7 eV, cf. Figure 6) to the semiquinone radical anion contact pair $\{M^{\bullet-}R_3Si\text{-}SiR_3^+\}$ (cf. Figure 25). In a consecutive slow reaction, presumably, the radical pair $\{R_3SiM^\bullet \cdots SiR_3^\bullet\}$ is generated, which by fast H transfer produces the hydroquinone mono(trimethylsilyl)ether R_3SiMH and

Chart 11

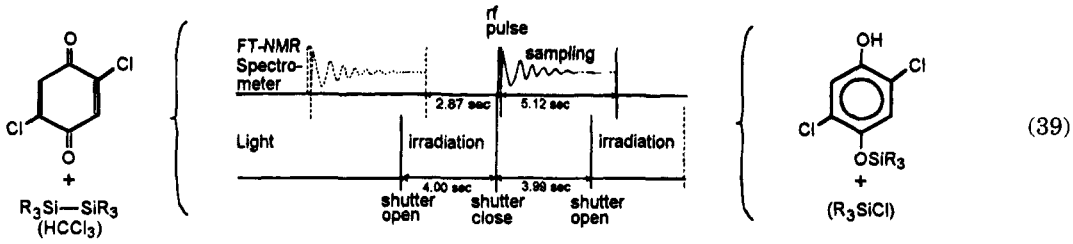

(39)

by Cl abstraction from the Cl_3CH solvent also produces R_3SiCl.[118]

Disappointingly, in most of the other numerous references obtained from the CAS on line search under the heading "organosilicon radical cations", mere speculation wins over attempts to prove a paramagnetic intermediate. Nevertheless, the following selected examples are presented in more detail.

Cyclovoltammetric measurements of silatranes $RSi(OCH_2CH_2)_3N$ in H_3CCN solution under reported aprotic conditions suggest partly reversible one-electron oxidation at low temperatures and high scan rates.[119] During oxidation of unsaturated six-membered ring hydrocarbons by iodine, ESR signals are reported as well as pyridine adduct formation to some of the radical cations generated.[120] For anodic olefin intramolecular coupling reactions including vinylsilane subunits, a proposal is put forward to view the initial addition "as if it occurred in a reversible radical-like fashion" without any experimental evidence for radical intermediates.[121] An analogous unjustified claim concerns the addition of silyl enol ethers to $(NH_4^+)_2[Ce^{+4}(NO_3^-)_6]$ oxidation products of allyl sulfides.[122] No experimental evidence supports the numerous assumptions for the proposed radical reaction pathway in a one-electron oxidation of 2,2-dimethyl-2-silaindane by $K_5^+Co^{+3}(W_{12}O_{40}^{-8})$.[123]

According to the CIDNP experiments with *p*-benzoquinones,[118] and other photochemical reactions of[124] or with[125] disilane derivatives,[39] the reaction will most likely proceed via radical cations in solvent cages. Further proof of paramagnetic species involved, however, still has to be provided.

Numerous publications concern photochemical reactions.[126-132] The desilylation of phenyl(trimethylsilyl)methyl ethers $RC_6H_4CH_2OSiR_3$ in the presence of electron acceptors as well as sensitizers is an example. Upon attempted spin-trapping of intermediates by adding 5,5-dimethyl-1-pyrroline *N*-oxide, ESR signals (although largely unresolved) were recorded.[126] In most other publications, however, efforts to prove paramagnetic intermediates by ESR[112] (Figure 25), by CIDNP,[118] or by other direct physical measurements have been, unjustifiably, replaced by a web of assumptions and speculations.[127-132] Therefore, interesting photochemical reactions such as those between silylalkylamines $R_2NCH_2SiR_3$ and cyclohexenones,[127] benzyl and other silane derivatives XCH_2SiR_3 with cyanohydrocarbons[128-130] as well as with aryl carbocations,[131] or the addition of allylsilanes to pyrrolinium salts[132] have to be either reinvestigated or no organosilicon radical cation intermediates should be claimed for fictious reaction mechanisms.

Summing up the proposals discussed for reactions via organosilicon radical cations in solution, both single electron transfer (SET) and photo electron transfer (PET) mechanisms are very likely to occur due to the low first vertical ionization energies of the neutral molecules (Figures 7, 14, and 15 as well as (18)–(23)). This point of view is further supported by the evidence compiled for well over 10 years that numerous types of reactions such as nucleophilic substitution, Diels/Alder addition, Wittig ylide synthesis, Claisen condensation, and especially carbanion and hydride anion acid/base exchanges do not necessarily proceed via electron pair attack, but often start with SET or PET redox exchanges.[133] Nevertheless, most of the selected literature reports reviewed above, which speculate about organosilicon radical cation participation, should be reinvestigated, for example, by short-time spectroscopic methods available nowadays to exclude additional possibilities for reaction pathways such as formation of reactive donor/acceptor complexes, radical dimerization, or dication generation within the solvent cages or on escape from them.[133]

V. Retrospective and Perspectives

The fascinating organosilicon radical cations reviewed for the last 6 years together with the previous basic knowledge can be characterized by their following prominent features.[1,2,16]

(1) The low effective nuclear charge of silicon centers in organic molecules stabilizes positive charges in their radical cation states (section I). Depending on the substituent perturbation pattern (section II), their first vertical ionization potentials in the gas phase as well as their oxidation potentials in solution, therefore, can be extremely low.

(2) In photoelectron spectroscopic gas phase investigations (section III) and ESR/ENDOR measurements in solution (section IV), which complement each other both as eigenvalue-determined (via Koopmans' theorem) and as eigenfunction squared correlated (via McConnell relation) as well a consequence of their different 10^{-15} and 10^{-7} s time scales, numerous relevant properties of organosilicon radical cations are accessible from energies for generation via spin and charge distribution to their dynamics.

(3) For main group element chemistry, striking substituent effects of partly bulky and kinetically shielding trialkylsilyl groups on π-systems and electron-rich lone-pair centers have been discovered, many of which are nowadays used in organic synthesis. The exploration of organosilicon radical cations has extended the range of the known, electron-deficient species from those with singly coordinate, triply bonded Si centers such as in $H_5C_6N{\equiv}Si^{\bullet+}$

(Figure 9) to 10-fold coordination such as in the sandwich π-complex $(R_5C_5)_2Si^{\bullet+}$ (Figure 18).

In the future, both academic research as well as industrial applications will vigorously explore the many unique properties of organosilicon radical cations, because they are easily predicted (e.g. from first ionization energies) and easily generated (e.g. by $AlCl_3$ addition to precursor solutions in H_2CCl_2) and because their properties can be easily rationalized (e.g. by quantum-chemical calculations). Special emphasis is anticipated in the following directions:[2]

(1) The steric and electronic effects of supersilyl substituents such as $((H_3C)_3Si)_3Si$, the huge van der Waals spheres of which are covered by each 27 hydrogens, will both kinetically shield and thermodynamically stabilize organosilicon radical cations and, therefore, should allow crystallization and structural characterization (Chart 8).

(2) Novel methods of measurements enlarging the scope of, for example, ionization−reneutralization and collisional activation mass spectroscopy or pulsed ESR techniques will widen the horizon of unique properties of organosilicon radical cations.

(3) The investigation of excited states might be explored by correlated quantum-chemical calculations including Rydberg states.[2] Furthermore, the evaluation of microscopic reaction pathways by energy hypersurface gradient methods coupled with all the experimental evidence available does offer interesting aspects.

(4) Last but not least, novel materials from doped, conducting polysilane polymers[134] to those with electron-rich heterocenters[135] open a window for future technical applications.

In closing, Galileo Galilei may be quoted also in reference to organosilicon radical cations: "Measure everything and the unmeasurable make measureable."

References

(1) Preceding Review I: Bock, H.; Solouki, B.; *Photoelectron Spectra of Silicon Compounds* in *The Chemistry of Organosilicon Compounds*; Patai, S., Rappoport, Z., Eds.; Wiley/Interscience: London, 1989; p 556−653, and all the references cited therein.

(2) Preceding Review II: Bock, H. Fundamentals of Silicon Chemistry: Molecular States of Silicon-Containing Compounds. *Angew. Chem.* **1989**, *101*, 1659−1682; *Angew. Chem. Int. Ed. Engl.* **1989**, *28*, *1627−1650* and references cited therein.

(3) Bock, H. *Molecular States and Molecular Orbitals. Angew. Chem.* **1977**, *89*, 631−655; *Angew. Chem. Int. Ed. Engl.* **1977**, *16*, 613−637, and references cited therein.

(4) Bock, H.; Ruppert, K.; Näther, C.; Havlas, Z.; Herrmann, H.-F.; Arad, C.; Göbel, I.; John, A.; Meuret, J.; Nick, S.; Rauschenbach, A.; Seitz, W.; Vaupel, T.; Solouki, B. Charge-Perturbed and Sterically Overcrowded Molecules; Perturbation Design, Preparation and Structures. *Angew. Chem.* **1992**, *104*, 564−595, *Angew. Chem. Int. Ed. Engl.* **1992**, *31*, 550−581 and references cited therein.

(5) The time scale in Figure 3 has been drawn according to the data given: Wiberg, N. *Lehrbuch der Anorganischen Chemie*, 91st−100th ed.; de Gruyter: Berlin, 1985; p 346.

(6) See, for example: Brundle, C. R. Baker, A. D. (Eds.) *Electron Spectroscopy: Theory, Techniques and Applications*; Academic Press: London, 1977−1984; Vol. 1−5, and references cited therein.

(7) Bock, H.; Solouki, B. *Real-Time Gas Analysis in Flow Systems. Angew. Chem.* **1981**, *93*, 425; *Angew. Chem. Int. Ed. Engl.* **1981**, *20*, 427.

(8) See, for example: Kurreck, H.; Kirste, B.; Lubitz, W. *Electron Spin Double Resonance Spectroscopy of Radicals in Solution*; VCH: Weinheim, 1988.

(9) Bock, H.; Dammel, R.; Roth, B. *Molecular State Fingerprints and Semiempirical Hypersurface Calculations*; ACS Symposium Series 232; American Chemical Society: Washington DC, 1983; pp 139−165.

(10) Bock, H.; Ensslin, W. *Angew. Chem.* **1971**, *83*, 435; *Angew. Chem. Int. Ed. Engl.* **1971**, *10*, 404. This publication on the discovery of electron delocalization in polysilanes is not cited by R. West, in his review on polysilanes in *The Chemistry of Organosilicon Compounds*; Patai, S., Rappoport, Z., Eds.; Wiley/Interscience: London, 1989; pp 1206−1240.

(11) Bock, H.; Ensslin, W.; Feher, F.; Freund, R. *J. Am. Chem. Soc.* **1976**, *98*, 668, and references cited therein.

(12) Bock, H., Hierholzer, B.; Kurreck, H, Lubitz, W. *Angew. Chem.* **1983**, *95*, 817; *Angew. Chem. Int. Ed. Engl.* **1983**, *22*, 787, and, especially, the details in *Angew. Chem. Suppl.* **1983**, *1088*.

(13) Bock, H.; Dammel, R. *Angew. Chem.* **1985**, *97*, 128; *Angew. Chem. Int. Ed. Engl.* **1985**, *24*, 111, and literature quoted. See also: Gross, G.; Michl. *J. Chem. Eng. News*, **1985**, *63*, No. 12, 31. Radziszewski, J. G.; Littmann, D.; Balaji, V.; Laszlo, F.; Gross, G.; Michl, J. *Organometallics* **1993**, *12*, 4816.

(14) See: Heilbronner, E., Bock, H. *The Model and its Application*; VCH Verlag: Weinheim, 1968−1970; Vol. I−III; Japanese translation: Hirokawa: Tokyo, 1973. English translation: Wiley-Interscience: London, 1975. Chinese translation: Kirin University Press: Kirin, 1983.

(15) Bock, H.; Ramsey, B. G. *Angew. Chem.* **1973**, *85*, 773; *Angew. Chem. Int. Ed. Engl.* **1973**, *12*, 734 and references cited therein.

(16) Bock, H.; Kaim, W. Organosilicon Radical Cations. *Acc. Chem. Res.* **1982**, *15*, 9, and the references cited therein.

(17) Bock, H.; Lechner-Knoblauch, U. *J. Organomet. Chem.* **1985**, *294*, 295.

(18) Bock, H.; Solouki, B.; Rosmus, P.; Dammel, R.; Hänel, P.; Hierholzer, B.; Lechner-Knoblauch, U.; Wolf, H. P. Recent Investigations on Short-lived Organosilicon Molecules and Molecular Ions. In *Organosilicon and Bioorganosilicon Chemistry*; Sakurai, H., Ed.; Ellis Horwood: Chichester, 1985; pp 45−73, and references cited therein.

(19) Raabe, G.; Michl, J. Multiple Bonds to Silicon in *The Chemistry of Organic Silicon Compounds*; Patai, S., Rappoport, Z., Eds.; Wiley: Chichester, 1989; pp 1015−1142, and literature quoted.

(20) See also: Bock, H.; Solouki, B.; Aygen, S.; Bankmann, M.; Breuer, O.; Dammel, R.; Dörr, J.; Haun, M.; Hirabayashi, T.; Jaculi, D.; Mintzer, J.; Mohmand, S.; Müller, H.; Rosmus, P.; Roth, B.; Wittmann, J.; Wolf, H.-P. *J. Mol. Struct.* **1988**, *173*, 31, and references cited therein.

(21) Solouki, B.; Rosmus, P.; Bock, H.; Maier, G. *Angew. Chem.* **1980**, *92*, 56, *Angew. Chem. Int. Ed. Engl.* **1980**, *19*, 51; see also: Bock, H.; Bowling, R. A.; Solouki, P.; Barton, T. J.; Burns, G. T. *J. Am. Chem. Soc.* **1980**, *102*, 429.

(22) Rosmus, P.; Bock, H.; Solouki, B.; Maier, G.; Mihm, G. *Angew. Chem.* **1981**, *93*, 616; *Angew. Chem. Int. Ed. Engl.* **1981**, *20*, 598.

(23) Murrell, J. N.; Kroto, H. W.; Guest, M. F. *J. Chem. Soc. Chem. Commun.* **1977**, *619*; cf. also Kroto, H. W.; Murrell, J. N.; Al-Derzi, A.; Guest, M. F. *Astrophys. J.* **1978**, *219*, 880, as well as Preuss, R., Buenker, R. J.; Peyer-Imhoff, S. D. *J. Mol. Struct.* **1978**, *49*, 171.

(24) Bock, H.; Dammel, R. *Angew. Chem.* **1987**, *99*, 518; *Angew. Chem. Int. Ed. Engl.* **1987**, *26*, 487.

(25) Batich, C.; Heilbronner, E.; Hornung, V.; Ashe, A. J.; Clark, D. T.; Cobley, U.T.; Kilcast, D.; Scanlan, I. *J. Am. Chem. Soc.* **1973**, *95*, 928.

(26) Ensslin, W.; Bock, H., Becker, G. *J. Am. Chem. Soc.* **1974**, *96*, 2757, and references cited therein.

(27) Bock, H., Kaim, W. *Chem. Ber.* **1978**, *111*, 3552 and Bock, H.; Kaim, W.; Rohwer, H.-F. *Ibid.* **1978**, *111*, 3573.

(28) Dewar, M. J. S.; Thiel, W. *J. Am. Chem. Soc.* **1977**, *99*, 4899, 4907.

(29) Dewar, M. J. S.; Zoebisch, E. G.; Healy, E. F., Stewart, J. B. *J. Am. Chem. Soc.* **1985**, *107*, 3902.

(30) Stewart, J. J. *J. Comput. Chem.* **1989**, *10*, 209, 221.

(31) Dewar, M. J. S.; Caoxian, *J. Organometallics* **1987**, *6*, 1486.

(32) Nelsen, S. F.; Hollinsed, W. C.; Kessel, C. R.; Calabrese, J. C. *J. Am. Chem. Soc.* **1978**, *100*, 7876.

(33) Nöth, H.; Winterstein, W.; Kaim, W.; Bock, H. *Chem. Ber.* **1979**, *112*, 2494.

(34) Luke, B. T.; Pople, A.; Krogh-Jespersen, M.-B.; Apeloig, Y.; Chandrasekar, J.; v. R. Schleyer, P. *J. Am. Chem. Soc.* **1986**, *108*, 260, 270, and the literature reviewed.

(35) Bock, H.; Kremer, M.; Dolg, M.; Preuss, H.-W. *Angew. Chem.* **1991**, *103*, 1200; *Angew. Chem. Int. Ed. Engl.* **1991**, *30*, 1186, and the references cited therein.

(36) Arduengo, A. J., III; Bock, H.; Chen, H.; Denk, K. M.; Dixon, D. A.; Green, J. C.C.; Herrmann, W. A.; Wagner, M.; West, R. *J. Am. Chem. Soc.* **1994**, *116*, 6641 and references cited therein. See also Denk, M.; Green, J. C.; Metzler, N.; Wagner, M. *J. Chem. Soc. Dalton Trans.* **1994**, *2405*.

(37) See, for example: Banholzer, W. F.; Lewis, N.; Ward, W. *J. Catal.* **1986**, *101*, 405.

(38) Shin, S. K.; Irikura, K. K.; Beauchamp, J. L.; Goddard, W. A., III *J. Am. Chem. Soc.* **1988**, *110*, 24.

(39) Wittel, K.; Bock, H. The Photoelectron Spectra of Organic Halogen Compounds In *The Chemistry of Functional Groups*,

Supplement D; Patai, S., Rappoport, Z., Eds.; Wiley-Interscience: Chichester, 1983; pp 1499–1603.
(40) Arduengo, A. J., III; Harlow, R. L.; Kline, M. *J. Am. Chem. Soc.* **1991**, *113*, 361 and Arduengo, A. J., III; Dias, H. V. R.; Harlow, R. L.; Kline, M. *Ibid.* **1992**, 114, 5530. See also: Arduengo, A. J., III; Dixon, D. A.; Kumashiro, K. K.; Lee, C.; Power, W. P.; Zilm, K. W. *J. Am. Chem. Soc.* **1994**, *116*, 6361 or Arduengo, A. J., III; Dias, H. V. R.; Dixon, D. A.; Harlow, R. L.; Kloster, W. T.; Koetzle, T. F. *Ibid.* **1994**, *116*, 6812.
(41) Herrmann, W. A.; Denk, M.; Behn, J.; Scherer, W.; Klingan, F.-H.; Bock, H.; Solouki, B.; Wagner, M. *Angew. Chem. Int. Ed. Engl.* **1992**, *11*, 1485.
(42) Denk, M.; Lennon, R.; Hayashi, R.; West, R.; Belyakow, A. V.; Verne, H. P.; Haaland, A.; Wagner, M.; Metzler, N. *J. Am. Chem. Soc.* **1994**, *116*, 2691.
(43) See: Bruno, G. In *Gli eroici furori*, Paris, 1585: "Se non e vero, e buon trovato" (if its not true, its well invented).
(44) Srinivas, R.; Böhme, D. K.; Schwarz, H.; *J. Phys. Chem.* **1993**, *97*, 13643.
(45) Hrusak, H.; Srinivas, R.; Böhme, D. K.; Schwarz, H. *Angew. Chem.* **1991**, *103*, 1396; *Angew. Chem. Int. Ed. Engl.* **1991**, *30*, 1323.
(46) Lim, K. P.; Lampe, F. W. *J. Chem. Phys.* **1992**, *96*, 2819.
(47) Johnson, R. D., III; Fang, E.; Hudgens, J. W. *J. Phys. Chem.* **1988**, *92*, 3880.
(48) Wright, S. C.; Cooper, D. L.; Sironi, M.; Raimondi, R.; Gerrat, J. *J. Chem. Soc. Perkin Trans. 2* **1990**, *369*.
(49) Hopkinson, A. C.; Lien, M. H. Can. *J. Chem.* **1989**, *67*, 991.
(50) Bock, H.; Meuret, *J. Organomet. Chem.* **1993**, *459*, 43
(51) Bock, H.; Meuret, J.; Stein, U. *J. Organomet. Chem.* **1990**, *398*, 65.
(52) Block, E.; Yencha, A. J.; Aslam, M.; Eswarakrishnan, V.; Luo, J.; Sano, A. *J. Am. Chem. Soc.* **1988**, *110*, 4748.
(53) Maroshina, M. Y.; Vlasova, N. N.; Voronkov M. G. *J. Organomet. Chem.* **1991**, *406*, 279.
(54) Nynlaszi, L.; Veszpremi, T.; Reffy, J. *J. Organomet. Chem.* **1993**, *445*, 29.
(55) See, for example: *Structure Correlation;* Bürgi, H.-B., Dunitz, J. D., Eds.; VCH Verlag: Weinheim, 1994; Vol. 2, Appendix A.
(56) Yoshida, J.; Maekawa, T.; Murata, T.; Matsunaga, S.; Iso, S. *J. Am. Chem. Soc.* **1990**, *112*, 1962.
(57) Bock, H.; Meuret, J.; Näther, C.; Krynitz, U. *Chem. Ber.* **1994**, *127*, 55, as well as *Tetrahedron Lett.* **1993**, *34*, 7553, and all the literature quoted. See also Gerson, F.; Krynitz, U.; Bock, H. *Angew. Chem.* **1969**, *81*, 786; *Angew. Chem. Int. Ed. Engl.* **1969**, *8*, 767.
(58) See: Bock, H.; Meuret, J.; Näther, C.; Ruppert, K. *Sterically Overcrowded Organosilicon Compounds and Their Properties in Organosilicon Chemistry—From molecules to Materials* Auner, N., Weis, J., Eds.; VCH Verlag: Weinheim, 1994; S. 11f, or *Phosphorus, Sulfur, Silicon, Rel. El.* **1995**, in press.
(59) Bock, H.; Meuret, J.; Bats, J. W.; Havlas, Z. *Z. Naturforsch. B* **1994**, *49*, 288.
(60) See, for example: Bock, H.; Göbel, I.; Näther, C.; Havlas, Z.; Gavezzotti, A.; Filippini, G. *Angew. Chem.* **1993**, *105*, 1823; *Angew. Chem.* **1993**, *32*, 1755.
(61) Bock, H.; Meuret, J.; Baur, R.; Ruppert, K. *J. Organomet. Chem.* **1993**, *446*, 113.
(62) Bock, H.; Meuret, J.; Schödel, H. *Chem. Ber.* **1993**, *126*, 2227.
(63) Bock, H.; Meuret, J.; Ruppert, K. *J. Organomet. Chem.* **1993**, *462*, 31.
(64) Bock, H.; Meuret, J.; Ruppert, K. *J. Organomet.* **1993**, *445*, 19.
(65) Sutherland, D. G. J.; Xiong, J. Z.; Liu, Z.; Sham, T. K.; Bancroft, G. M.; Baines, K. M.; Tan, K. H. *Organometallics* **1994**, *13*, 3671.
(66) Jutzi, P.; Hoffmann, U.; Kanne, D.; Krüger, C., Blom, R.; Gleiter, R.; Hyla-Krispin, I. *Chem. Ber.* **1989**, *122*, 1629.
(67) Seyfert, D.; Büchner, K. D.; Rees, W. S.; Wesemann, L.; Davis, W. M.; Bukalov, S. S.; Leites, L. A.; Bock, H.; Solouki, B. *J. Am. Chem. Soc.* **1993**, *115*, 5386, and literature cited.
(68) Lichtenberger, D. L.; Rai-Chaudhuri, A., *J. Am. Chem. Soc.* **1989**, *111*, 3583 and **1990**, *112*, 2492.
(69) Lichtenberger, D. L.; Rai-Chaudhuri, A. *Inorg. Chem.* **1990**, *29*, 975 and *Organomet.* **1990**, *9*, 1686.
(70) Lichtenberger, D. L.; Rai-Chaudhuri, A. *J. Am. Chem. Soc.* **1991**, *113*, 2923.
(71) Ciliberto, E.; DiBella, S.; Giulino, A.; Fragala, I.; Petersen, J. L.; Marks, T. J. *Organomet.* **1992**, *11*, 1727.
(72) Gassmann, P. G.; Deck, P. A.; Winter, C. H.; Dobbs, D. A.; Cao, D. H. *Organomet.* **1992**, *11*, 959.
(73) Andersen, R. A.; Faegri, K.; Green, J. C.; Haaland, A.; Lappert, M. F.; Leung, W.-P.; Rypdal, K. *Inorg. Chem.* **1988**, *27*, 1782. See also Andersen, R. A.; Berg, D. J.; Fernholt, L.; Faegri, K.; Green, J.C.; Haaland, A.; Lappert, M. F.; Leung, W.-P.; Rypdal, C. *Acta Chem. Scand Sect. A.* **1988**, *42*, 554.
(74) Berkowitz, J. *Acc. Chem. Res.* **1989**, *22*, 413.
(75) Bock, H.; Kremer, M.; Schmidbaur, H. *J. Organomet. Chem.* **1992**, *429*, 1.
(76) Grabandt, O.; de Lange, C. A.; Mooyman, R.; Vernooijs, P. *Chem. Phys. Lett.* **1991**, *184*, 221.
(77) Stüger, H.; Janoschek, R. *Phosphorus, Sulfur, Silicon Rel. El.* **1992**, *68*, 129.
(78) Werstiuk, N. H.; Brook, M. A.; Hülser, P. *Can. J. Chem.* **1988**, *66*, 1430.
(79) Peel, J. B.; Dianxun, W. *J. Chem. Soc. Dalton Trans.* **1988**, *1963*. See also Sidorkin, V. F.; Balakhchi, G. K. *Struct. Chem.* **1994**, *5*, 189.
(80) Veszpremi, T.; Pasinszki, T.; Nyulaszi, L.; Csonka, G.; Barta, I. *J. Mol. Struct.* **1988**, *175*, 411. See also Pasinszki, T., Reffy, J.; Veszpremi, T. *Monatsh. Chem.* **1992**, *123*, 949.
(81) Gleiter, R.; Pfeifer, K.-H.; Baudler, M.; Scholz, G.; Wettling, T.; Regitz, M. *Chem. Ber.* **1990**, *123*, 757.
(82) Distefano, G.; Zanathy, L.; Szepes, L.; Breunig, H. J. *J. Organomet. Chem.* **1988**, *338*, 181.
(83) Nagy, A.; Green, J. C.; Scepes, L.; Zanathy, L. *J. Organomet. Chem.* **1991**, *419*, 27.
(84) Gleiter, R.; Schäfer, W. M Krennrich, G.; Sakurai, H. *J. Am. Chem. Soc.* **1988**, *110*, 4117.
(85) Bozek, J. D.; Bancroft, G. M.; Tan, K. H. *Phys. Rev. A.* **1991**, *43*, 3597 or Bozek, J. D.; Cutler, J. N.; Bancroft, J. M.; Coatsworth L. L.; Tan, K. H.; Yang, D. S. *Chem. Phys. Lett.* **1990**, *165*, 1.
(86) See, for example: Frey, R. D.; Davidson, E. R. *J. Chem. Phys.* **1988**, *89*, 4227, Kudo, T.; Nagase, S. *Chem. Phys.* **1988**, *122*, 233 or Caballot, R.; Catala, J. A.; Problet, J. M. *Chem. Phys. Lett.* **1986**, *130*, 278.
(87) For reviews on matrix isolation techniques, see, for example: Shiotani, M. *Magn. Reson. Rev.* **1987**, *12*, 333 or *Radical Ionic Systems*; Lund, A.; Shiotani, M., Eds.; Kluwer Academic Publishers: Dordrecht, 1991.
(88) See, for example: Walther, B. W.; Williams, D. *J. Chem. Soc. Chem. Commun.* **1982**, *270* and lit. cit.
(89) Bonazzola, L.; Michaut, J. P.; Roncin, J. *New J. Chem.* **1992**, *16*, 489.
(90) See, for example: Kira, M.; Nakazawa, H.; Sakurai, H. *J. Am. Chem. Soc.* **1983**, *105*, 6983, as well as *Chem. Lett.* **1985**, *1845*.
(91) Takahashi, O.; Morihashi, K.; Kiruchi, O. *Bull. Chem. Soc. Jpn.* **1991**, *64*, 1178.
(92) See, for example: Kira, M.; Nakazawa, H.; Sakurai, H. *Chem. Lett.* **1985**, *1841*, 1845 and 1986, 497.
(93) Knight, L. B.; Winiski, M.; Kudelko, P.; Arrington, C. A. *J. Chem. Phys.* **1989**, *91*, 3368.
(94) Ohta, N.; Kikawa, S.; Ichikawa, T. *J. Chem. Soc. Perkin Trans.* **1993**, *945*.
(95) Shiotani, M.; Komaguchi, K.; Oshita, J.; Ishikawa, M.; Sjöqvist, L. *Chem. Phys. Lett.* **1992**, *188*, 93.
(96) Komaguchi, K.; Shiotani, M.; Ishikawa, M., Sasaki, K. *Chem. Phys. Lett.* **1992**, *200*, 580.
(97) Butcher, E.; Rhodes, C. J.; Standing, M.; Davidson, R. S.; Bowser, R. *J. Chem. Soc. Perkin Trans.* **1992**, *1469*.
(98) Rhodes, C. J. *J. Organomet. Chem.* **1988**, *356*, 17.
(99) Rhodes, C. J. *J. Chem. Soc. Perkins Trans. II* **1992**, *235* and *J. Chem. Res. Synop.* **1989**, *28*.
(100) Graalmann, O.; Hesse, M.; Khingebiel, U.; Clegg, W.; Haase, M.; Sheldrick, G. M. *Angew. Chem.* **1983**, *95*, 630; *Angew. Chem. Int. Ed. Engl.* **1983**, *22*, 621.
(101) See, for example: Bock, H.; Jaculi, D., *Z. Naturforsch. B* **1991**, *46*, 1091.
(102) Bock, H.; Kaim, W.; Kira, M.; West, R. *ibid.* **1979**, *101*, 7667, and the literature cited therein, especially, Carberry, E.; West, R.; Glass, E. E. *J. Am. Chem. Soc.* **1969**, *91*, 5446.
(103) See, for example: Kudo, T.; Nagase, S. *Chem. Phys. Lett.* **1989**, *164*, 217.
(104) Bock, H.; Meuret, J.; Ruppert, K.; *Chem. Ber.* **1993**, *126*, 2237.
(105) Hausen, H.-D.; Kaim, W. *Z. Naturforsch. B* **1988**, *43*, 82.
(106) Hausen, H.-D.; Bessenbacher, C.; Kaim, W. *Z. Naturforsch. B* **1988**, *43*, 1988.
(107) Lichtblau, A.; Hausen, H.-D.; Kaim, W. *Z. Naturforsch. B* **1993**, *48*, 713.
(108) Bessenbacher, C.; Kaim, W. *Z. Naturforsch. B* **1989**, *44*, 511.
(109) Kaim, W.; Lichtblau, A.; Hausen, H.-D. *J. Organomet. Chem.* **1993**, *456*, 167.
(110) Bessenbacher, C.; Kaim, W. *J. Chem. Soc. Chem. Commun.* **1989**, *469*.
(111) Björgvinsson, M.; Heinze, T.; Roesky, H. W.; Pauer, F.; Stalke, D.; Sheldrick, G. M. *Angew. Chem.* **1991**, *103*, 1671; *Angew. Chem. Int. Ed. Engl.* **1991**, *30*, 1677.
(112) Bock, H.; How Do Medium-Sized Molecules Actually React? *Polyhedron* **1988**, *7*, 2429 and *Rev. L'Actualité Chim.* **1986/3**, *33*.
(113) See, for example: Van den Winkel, Y.; van Baar, B. L. M.; Bickelhaupt, F.; Kulik, W.; Sierakowski, C.; Maier, G. *Chem. Ber.* **1991**, *124*,185.
(114) Srinivas, R.; Hrusak, J.; Sülzle, D.; Böhme, D. K.; Schwarz, H. *J. Am. Chem. Soc.* **1992**, *114*, 2802 and Böhme, D. K.; Wlodek, S.; Winel, H. *Ibid.* **1991**, *113*, 6396.
(115) Srinivas, R.; Böhme, D. K.; Hrusak, J.; Schröder, D.; Schwarz, H. *J. Am Chem. Soc.* **1992**, *114*, 1939, as well as Hrusak, J.; Srinivas, R.; Böhme, D. K.; Schwarz, H. *Angew. Chem.* **1991**, *103*, 1396; *Angew. Chem. Int. Ed. Engl.* **1991**, *30*, 1323.

(116) Srinivas, R.; Sülzle, D.; Koch, W.; Depuy, C. H.; Schwarz, H. *J. Am. Chem. Soc.* **1991**, *113*, 5970.
(117) Stöckigt, D.; Goldberg, N.; Hrusak, J.; Sülzle, D.; Schwarz, H. *J. Am. Chem. Soc.* **1994**, *116*, 8300.
(118) Cf.e.g. Igarashi, M.; Ueda, T.; Wakasa, M.; Sakaguchi, Y. *J. Organomet. Chem.* **1991**, *421*, 9, and literature cited therein.
(119) Broka, K.; Stradius, J; Glezer, V.; Zelcans, G.; Lukevics, E. J. Electroanal. Chem. 1993, 351, 199. Cf. Also Brodskaya, E. I.; Voronkov, M. G.; Belyaeva, V.V.; Baryshok, V. P.; Lazareva, N. *F. Zh. Obshch. Khim.* **1993**, *63*, 2252 (*Chem. Abstr.* **1993**, *119*, 205462*r*).
(120) Sirimanne, S. R.; Li, Z.; Vander Veer, D. R.; Tolbert, L. M. *J. Am. Chem. Soc.* **1991**, *113*, 1766, and the literature cited.
(121) Hudson, C. M.; Moeller, K. D. *J. Am. Chem. Soc.* **1994**, *116*, 3347.
(122) Narasaka, K.; Okauchi, T. *Chem. Lett.* **1991**, *515*
(123) Baciocchi, E.; Bernini, R.; Lanzalunga, O. *J. Chem. Soc. Chem. Commun.* **1993**, *1691*.
(124) Nakadaira, Y.; Sekiguchi, A.; Funada, Y.; Sakurai, H. *Chem. Lett.* **1991**, *327*.
(125) Mizuno, K.; Nakanishi, K.; Chosa, J.; Otsuji, Y. *J. Organomet. Chem.* **1994**, *473*, 35.
(126) Abraham, W.; Glänzel, A.; Stösser, R.; Grummt, U.-W.; Köppel, H. *J. Photochem. Photobiol. A* **1990**, *51*, 359.
(127) Hasegawa, E.; Xu, W.; Mariano, P. S.; Yoon, U.-C.; Kim, J.-U. *J. Am. Chem. Soc.* **1988**, *110*, 8099, as well as Yoon, U. C.; Kim, Y. C.; Choi, J. J.; Kim, D. U.; Mariano, P. S.; Cho, I.-S.; Jeon, Y. T. *J. Org. Chem.* **1992**, *57*, 1422.
(128) D'Alessandro, N.; Fasani, E.; Mella, M.; Albini, A. *J. Chem. Soc. Perkin Trans.* **1991**, *1977*; Mella, M.; d'Allessandro, N.; Freccero, M.; Albini, A. *Ibid.* **1993**, *115* or d'Allessandro, N.; Albini, A.; Mariano, P. S. *J. Org. Chem.* **1993**, *58*, 937.
(129) Dinnocenzo, J. P.; Farid, S.; Goodman, J. L.; Gould, I. R.; Todd, W. P.; Mattes, S. L. *J. Am. Chem. Soc.* **1989**, *111*, 8973 or *Tetrahedron Lett.* **1993**, *34*, 2863.
(130) Heidbreder, A.; Mattay, *J. Tetrahedron Lett.* **1992**, *33*, 1973.
(131) Azarani, A.; Berinstain, A. B.; Johnston, L. J.; Kazanis, S. *J. Photochem. Photobiol.* **A 1991**, *57*, 175.
(132) Haddaway, K.; Somekawa, K.; Fleming, P.; Tossell, J. A.; Mariano, P. S. *J. Org. Chem.* **1987**, *52*, 4239.
(133) Kaim, W. One-Electron Transfer: Farewell to Electron Pair Mechanisms, *Nachr. Chem. Tech. Lab.* **1984**, *32*, 436, and literature quoted.
(134) Cf.e.g. Irie, S.; Oka, K.; Irie, M. *Macromolecules* **1988**, *21*, 110.
(135) See, for example: Yi, S. H.; Nagase, J.; Sato, H. *Synth. Met.* **1993**, *58*, 353.

CR941092B